



DEPARTAMENTO DE CIÊNCIAS DA VIDA

FACULDADE DE CIÊNCIAS E TECNOLOGIA
UNIVERSIDADE DE COIMBRA

Characterization of human umbilical cord matrix mesenchymal stem cells isolated and cultured on tunable hydrogel-based platforms

Dissertação apresentada à Universidade de Coimbra para cumprimento dos requisitos necessários à obtenção do grau de Mestre em Biologia Celular e Molecular, realizada sob a orientação científica do Doutor Mário Grãos (Biocant) e do Professor Doutor Carlos Jorge Alves Miranda Bandeira Duarte (Universidade de Coimbra)

Este trabalho é financiado por Fundos FEDER através do Programa Operacional Fatores de Competitividade – COMPETE e por Fundos Nacionais através da FCT – Fundação para a Ciência e a Tecnologia no âmbito do projeto FCOMP-01-0124-FEDER-021150 (referência FCT: PTDC/SAU-ENB/119292/2010)

Plácido Júnio da Paixão Pereira

2013

Agradecimentos / Acknowledgements

Primeiro de tudo gostaria de agradecer ao meu primeiro orientador Mário Grãos por toda a sua predisposição a ajudar e orientar durante todo o projecto, por todo o apoio que me deu e pela paciência e compreensão que teve comigo durante o ultimo ano.

Em segundo eu gostaria de agradecer às minhas colegas do laboratório Tânia Loureiro, Manuela Lago e Catarina Domingues por toda a ajuda que me deram durante o ultimo ano e por terem sido umas excelentes amigas e colegas, especialmente a Tânia e à sua paciência.

Gostaria de agradecer ao Professor Carlos Duarte por ter aceite participar no projecto enquanto orientador mesmo que para isso tivesse de se deslocar de Cantanhede a Coimbra.

Queria agradecer ao principais financiadores deste projecto sem os quais não teria sido possivel nomeadamente à FEDER através do Programa Operacional Fatores de Competitividade – COMPETE e à FCT – Fundação para a Ciência e a Tecnologia no âmbito do projeto FCOMP-01-0124-FEDER-021150 (referência FCT: PTDC/SAU-ENB/119292/2010)

Queria ainda agradecer à Crioestaminal Saúde e Tecnologia S.A. pelas amostras de cordões umbilicais e às suas duas funcionárias regulares do laboratório de Biologia Celular Ana e Sofia pelas infindáveis horas que conversamos na sala de cultura

Queria também agradecer ao Dr. Artur Paiva e ao Tiago Carvalheiro do CHC pela ajuda na caracterização fenotípica das MSCs e ao Professor Lopes da Silva da universidade de Aveiro pela ajuda na caracterização dos hidrogéis de poliacrilamida.

Queria ainda agradecer a todo o pessoal do Biocant que me ajudou e me apoiou, nomeadamente à Susana, ao Grilo, a Catarina, ao João, Curto, Rita e Ana Sofia.

Queria agradecer à minha namorada Juliana pela paciência e compreensão que teve comigo assim como pelo seu apoio durante estes últimos 2 anos de mestrado os quais sem a sua companhia teriam sido muito mais difíceis.

Queria agradecer finalmente a minha família principalmente ao meu Pai e a minha Mãe por todo o apoio que me deram a todos os níveis e que sem eles nada disto teria sido possível

Abstract

It is described that Mesenchymal Stem Cells (MSCs) are extremely responsive to modulation by mechanotransduction (Chen, 2008; Eyckmans et al., 2011; Moore et al., 2010), namely by expressing typical lineage-specific genes when cultured *in vitro* on substrates with mechanical properties similar to those of the target tissues. Namely, MSCs express neural genes when cultured on substrates compliant with neural tissues (1-10 kPa) (Engler et al., 2006). It has also been described that these cells seem to retain some memory related to the stiffness of the substrates in which they were previously cultured on (Tse et al., 2011).

Typically, MSCs are isolated and cultured on polystyrene culture dishes (Tse et al., 2011) and eventually transferred onto compliant substrates after several passages to assess their plasticity in terms of lineage-specific expression markers, as reported in case of osteogenic-, myogenic- or neural-like commitment (Engler et al., 2006). Nevertheless, MSCs might retain memory (Tse et al., 2011) from the extremely high stiffness of polystyrene, possibly restraining their full potential in terms of lineage commitment.

It is of interest to understand what would be the effect of isolating MSCs directly on substrates with stiffness similar to that of neural tissues in terms of their potential to express neural markers. We propose to isolate and culture human umbilical cord matrix MSCs directly on softer substrates, namely hydrogels compliant with neural tissue (1 to 10KPa). As a control, part of the umbilical cord matrix of every sample will be used to isolate MSCs using normal tissue-culture polystyrene plates (the typical isolation and culture protocol) (Secco et al., 2008) and then transferred onto similar hydrogels after several passages on polystyrene (P1-P5), to address if prolonged culture on hard polystyrene is restraining their capacity to express neural markers later on. To promote the attachment of MSCs onto the hydrogels for isolation and culture, these will be covalently functionalized with collagen (Engler et al., 2006) and Fibronectin.

We optimized a new hMSCs isolation protocol for MSCs from UCM, allowing us to obtain naive hMSCs with a more homogenous population when compared to the isolation in TCPs. The PA hydrogels used for the isolation are commonly used in mechanotransduction experiments, but neither this specific formulation neither the

isolation of hUCM-MSCs was ever done before in PA hydrogels to the best of our knowledge. We can conclude that FN together with substrate stiffness have an important role in the initial proliferation impulse of hMSCs when cultured on soft substrates, namely at 10kPa (Figure 17). Preliminary results (Figure 18, 19 and Table III) show what appears to be a more naive and more homogenous population of hMSCs isolated and cultured on the PA hydrogels. Finally, it seems that neural markers (B-III tubulin, Nestin, O4 and GFAP) are more expressed in differentiating hMSCs plated on soft hydrogels than on plastic for hMSCs expanded for 5 passages on plastic. In terms of hMSCs isolated exclusively on PA hydrogels, the differences between these and hMSCs isolated on plastic were very evident, but O4 seems to be more expressed in cells isolated on soft PA hydrogels.

Key words: MSCs, oligodendroglia, mecanotransduction, matrix elasticity, lineage specification, differentiation.

Resumo

Está descrito que as células mesenquimais estaminais (MSCs) são extremamente reactivas à modulação por mecanotransdução (Chen, 2008; Eyckmans et al., 2011; Moore et al., 2010), nomeadamente através da expressão típica de genes específicos da linhagem de certos tecidos quando cultivados *in vitro* em substratos com propriedades mecânicas similares às dos mesmos. Nomeadamente, as MSCs quando cultivadas em substratos com rigidez semelhante a dos tecidos neuronais (1-10 kPa) expressam genes neuronais (Engler et al., 2006). Também tem sido descrito que estas células parecem reter algum tipo de memória relacionada com a rigidez dos substratos em que estiveram cultivadas (Tse et al., 2011).

Normalmente as MSCs são isoladas e cultivadas em placas de cultura de poliestireno e depois de várias passagens transferidas para substratos apropriados para determinar a sua plasticidade em termos de expressão de marcadores de linhagem celular específica, como já descrito nos casos de “compromisso” dos tipos osteogénico, miogénico e neurogénico (Engler et al., 2006).

No entanto, as MSCs podem reter alguma “memória” do contacto anterior com o poliestireno de rigidez extremamente alta quando comparada a de tecidos humanos, possivelmente diminuindo o potencial em termos de diferenciação (em termos de compromisso com as diferentes linhagens celulares).

É do nosso interesse perceber quais serão os efeitos de isolar as MSCs directamente em substratos com rigidez similar a dos tecidos neuronais em termos do seu potencial para expressar marcadores neuronais. Propomos então isolar e cultivar MSCs da matriz do cordão umbilical humano (hUCM) directamente em substratos mais moles, nomeadamente, hidrogéis semelhantes em rigidez ao tecido neuronal (1 a 10 kPa). Como controlo parte da matriz do cordão umbilical de cada amostra irá ser usado para isolar MSCs usando o protocolo base em placas de cultura de tecidos de poliestireno (TCPs) (Secco et al., 2008) sendo depois transferidas para hidrogéis similares após algumas passagens em poliestireno (P1-P5), para verificar se a cultura prolongada em poliestireno rígido é um factor de restrição na sua capacidade de expressar marcadores neuronais após a cultura em plástico. Para promover a adesão das MSCs aos hidrogéis para a isolamento e cultura, estes vão ser covalentemente funcionalizados com colagénio (Engler et al., 2006) e em alguns casos fibronectina.

Conseguimos otimizar um novo protocolo para isolar MSCs humanas do cordão umbilical, permitindo-nos obter uma população de MSCs humanas indiferenciadas mais homogênea quando comparado com o protocolo de isolamento em TCPs. Os hidrogéis de poliacrilamida (PA) usados para a isolamento já são utilizados comumente em experiências de mecanotransdução, mas tanto esta formulação dos hidrogéis como a isolamento das hUCM-MSCs em hidrogéis, nunca foi feito antes à luz do nosso conhecimento. Podemos concluir que a FN juntamente com a rigidez do substrato tem um papel importante na proliferação inicial das MSCs humanas quando cultivadas em substratos moles, nomeadamente a 10kPa (Figura 17). Os resultados preliminares (Figuras 18, 19 e tabela III) mostram o que parece ser uma população de MSCs humanas mais indiferenciada e mais homogêneas quando isoladas e cultivadas nos hidrogéis de PA. Finalmente, parece-nos que certos marcadores neuronais (B-III tubulin, Nestin, O4 e GFAP) estão mais expressos nas células já em diferenciação cultivadas nos hidrogéis moles do que nas cultivadas e em diferenciação no plástico (TCP), isto para as células expandidas durante 5 passagens no plástico (TCPs). Em relação as MSCs humana isoladas exclusivamente nos hidrogéis de PA as diferenças entre estas e as MSCs isoladas no plástico não são muito evidentes, mas parece que o O4 está mais expresso nas células isoladas em hidrogéis moles de PA.

Palavras-chave: MSCs, oligodendroglia, mecanotransdução, elasticidade da matriz, compromisso de linhagens celulares, diferenciação.

Table of contents

Acknowledgements	i
Abstract	iii
Resumo	v
Table of contents	viii
List of figures	xi
List of tables	
List of abbreviations	
Chapter I	1
I – Introduction	3
I.1. Mesenchymal stem cells (MSCs)	3
I.1.1 - Sources of MSCs	3
I.1.2 - <i>In vitro</i> characterization of MSCs	4
I.1.2.1 - Immunophenotype	5
I.1.2.2 - CFU-F and proliferation capacity	5
I.1.2.3 -Multilineage differentiation capacity	5
I.2. - Mechanotransduction and its implications in cellular fate	6
I.2.1 -Mechanotransduction and mechanosensors	9
I.2.2 -Extracellular matrix and integrin-based mechanotransduction	
Mechanisms	11
I.2.2.1 -Mechanisms of Rigidity Sensing	11
I.2.3 -Mechanotransduction and Stem Cells	15
I.2.3.1 - Mechanotransduction and MSCs differentiation	15
I.2.3.1.1-Stiffness effect on Neuronal and Glial differentiation	19
I.2.3.2-Manipulation and measurement of cellular forces in MSCs	21
I.3 - Project rationale and experimental approach	24
I.3.1 -Typical MSCs Isolation	24
I.3.2 -Durotaxis, Tissue Elasticity and MSCs “memory”	24
I.3.3 - Effects of the stiffness on the MSCs stemness genes	27

I.4 – Objectives	29
Chapter II	31
II – Materials and Methods	33
II.1 - Materials	33
II.1.1 - Cell culture	33
II.1.2 – Polyacrylamide hydrogels	33
II.1.3 - Immunocytochemistry	33
II.1.4 – Biological material	34
II.1.4.1 - Umbilical Cord Samples	34
II.1.4.2 - human Mesenchymal Stem Cells (hMSCs)	34
II.2 - Methods	34
II.2.1 – Isolation of Mesenchymal Stem Cells (MSCs) from Umbilical Cord Fragments (UCFs) in Tissue Culture Plates (TCPs) and Polyacrylamide hydrogels	34
II.2.2 - Cell culture	35
II.2.3 - Cryopreservation of MSCs	35
II.2.4 - Phenotypic characterization of UCM-MSCs	35
II.2.5 - Preparation of polyacrylamide hydrogels	36
II.2.6 Differentiation protocols	38
II.2.6.1 adapted from Engler, et al. 2006	38
II.2.7 - Rheological characterization of polyacrylamide hydrogels	38
II.2.8 - Immunocytochemistry	39
II.2.9 - Statistical analysis	39
Chapter III	41
III – Results	43
III.1 – Rheological Characterization of Polyacrylamide Hydrogels	43
III.2 – Cell Adhesion to Polyacrylamide Hydrogels functionalized with Collagen I (COL-1)	44
III. 3 – hMSCs Proliferation Assay	46
III.4 – Isolation and Proliferation of MSCs from Human Umbilical Cord Isolation of hMSC from the Wharton Jelly on Polyacrylamide Hydrogels	47
III.5 - Immunophenotypic characterization of UCM-MSC	48

III. 6 – Influence on MSCs specification by matrix elasticity	51
Chapter IV	58
IV – Discussion and Conclusion	60
Discussion	60
Conclusion	67
References	69

List of figures

Figure 1 | Mechanotransduction in a Cell-ECM Unit: Center image– A cell connected to another cell and to the ECM. Center image (A) and (D)- show where mechanotransduction in the cell-ECM unit occurs. The “blue lines” represent actomyosin filaments, “green lines” embody intermediate filaments and the “red lines” correspond to microtubules in all panels. Integrins are represented by the “blue structures” linking the cell with the ECM (D); Center “nucl.” – nucleus; (A) - Mechanotransduction at adherens junctions; (A), LEFT Shows different cell-cell junctions – “Tight” is for tight junctions. “GAP” is for Gap junctions. “Desm” is for desmosomes. “AJ” is for Adherens junctions. (A), RIGHT: Shows the Molecular structure of an AJ: E-cad: E-Cadherin, a: Alpha Catenin, b: Beta Catenin, p120: p120 Catenin, v: Vinculin; (B) -Mechanoreceptors at the cell membrane. Deformation of the plasma membrane by the fluid flow or stretching, leads to activation of ion channels resulting in an ions influx. Furthermore fluid flow directly impacts glycocalyx and cilia movement which triggers diverse downstream signaling cascades. Mechanical forces also mediate growth factor receptor (GR) clustering and endocytosis, and thus affect GR signal transduction as well; (C) - Mechanotransduction at the nucleus. Intermediate filaments and microtubules are interconnected with the nucleus and surrounding organelles (Golgi apparatus, Mitochondria, rough and smooth endoplasmic reticulum). Nesprins (N) bind the nucleus with the actomyosin cytoskeleton. With the change in cell shape and contractility there is an alteration to spatial localization of organelles which may lead to a conformational change in the nuclear pores. (D) - Mechanotransduction at the focal adhesion (FA). (D, LEFT): Nascent adhesions (NA), focal complexes (FXs) and focal adhesions (FA), undergo through a maturing process controlled by actomyosin contractility which can be modified by stiffness, shape or external application of force. (D, RIGHT): molecular structure of FA. α/β : alpha and beta sub-units of integrins, Pax: paxillin, F: Force delivered by actomyosin contraction. The clustering of integrins may induce RhoA signaling which leads to an increase of myosin contractility and an unfolding of proteins. Adapted from Eyckmans et al., 2011.

Figure 2| Proteins related to the mechanosensory in Integrin-Mediated Rigidity Sensing. The yellow boxes highlight the proteins which bind directly to the depicted domains. (A) FAK activity is regulated by mechanical force but does not bind integrins or actin directly. (B) Stretching the p130Cas domain exposes its 15 tyrosine residues. (C) Stretching of talin's rod domain exposes vinculin binding sites (del Rio et al., 2009). (D) Extension of filamin immunoglobulin repeats (labeled 1–24) has been shown by AFM (Furuie et al., 2001) and could regulate the binding of proteins. (E) α -actinin forms antiparallel dimers; mechanical force could regulate this dimerization or its association with other proteins. Adapted from Moore et al., 2010.

Figure 3| The Rigidity Sensing Cycle. In this rigidity sensing cycle scheme it is shown the correlation between mechanosensory events as integrin/ECM catch bond formation, stretching of talin (that recruits vinculin and therefore reinforces the adhesion) and stretching of FAK, leading to the disassembly and recycling of the adhesion, by the activation of its kinase domain. Adapted from; Moore et al., 2010

Figure 4| Tissue Elasticity. Range of stiffness measured by the elastic modulus, E , of some human solid tissues. Adapted from Engler et al., 2006.

Figure 5| Images depicted on A) and B) quantify the morphological changes (mean \pm SEM) versus stiffness, E : shown are (A) cell branching per length of primary mouse neurons, MSCs, and blebbistatin-treated MSCs and (B) spindle morphology of MSCs, blebbistatin-treated MSCs, and mitomycin-C treated MSCs (open squares) compared to C2C12 myoblasts (dashed line). Furthermore in C) MSCs change their morphology developing increasingly branched, spindle, or polygonal shapes, respectively, when cultured on matrices with the elastic modulus (E) respectively in the range typical of brain (0.1–1 kPa), muscle (8–17 kPa), or stiff crosslinked-collagen matrices (25–40 kPa). Blebbistatin blocks morphology changes due to stiffness (<2-fold different from naive MSCs) and mitomycin-C inhibits cell proliferation. Adapted from Engler et al., 2006.

Figure 6| Microarray profiling of MSC transcripts in cells cultured on 0.1, 1, 11, or 34 kPa matrices with or without blebbistatin treatment. Results are normalized to actin levels and then normalized again to expression in naive MSCs, yielding the fold increase at the bottom of each array. Neurogenic markers (left) are clearly highest on 0.1–1 kPa gels, while myogenic markers (center) are highest on 11 kPa gels and osteogenic markers (right) are highest on 34 kPa gels. Adapted from Engler et al., 2006).

Figure 7| A) Immunofluorescence images of B-III tubulin and NFH in branched extensions of MSCs on soft matrices ($E \approx 1$ kPa). Scale bars are 5 μ m. B) B-III tubulin, NFH, and P-NFH all localize to the branches of MSCs on the softest substrates with $E < 1$ kPa (mean \pm SEM). Nestin, B-III tubulin, MAP2, and NFL Western blotting (inset) confirms expression only on soft gels (GL = Glass). Adapted from Engler et al., 2006.

Figure 8| Protein profile dependent of elasticity. The neuronal cytoskeletal marker (small arrows) B-III tubulin, the muscle transcription factor MyoD1 (filled arrow) and the osteoblast transcription factor CBFA1 (empty arrow) are only expressed on the soft, myogenic and stiff matrices respectively. Scale bar is 5 μ m. Adapted from Engler et al., 2006.

Figure 9| Characterization of neural-like lineage differentiation of hMSCs in 3-D scaffolds. The qRT-PCR results for representative neural lineage specific genes. D7= 7 days. D14 = 14 days. EDC_0.1% = ≈ 1 kPa. EDC_2.0% = ≈ 10 kPa ($n = 3$, * $P < 0.1$, ** $P < 0.05$) (Adapted from Her et al., 2013).

Figure 10| Figure representing analysis of microposts heights (L) by finite-element method (FEM) each bending in response to applied horizontal traction force (F) of 20 nN. Adapted from Fu et al., 2010.

Figure 11| Images of mitomycin C-treated MSCs on gradient hydrogels (with stiffness gradient, ≈ 1 to 15 kPa) and their spatial distribution. Hoescht 33342 (blue) and phalloidin (red)-stained mitomycin C-treated MSCs plated at 250 cells/cm², illustrate

the change in distribution with time. Scale bar is 56.5 μm . Adapted from Tse and Engler, 2011.

Figure 12| MSCs cultured on 1 and 11 kPa static (top) and gradient (bottom) hydrogels and stained for β -III-tubulin (red) (neuronal marker) and MyoD (green) (myogenic marker). Open arrowheads indicate cells expressing either β -III-tubulin or MyoD while filled arrowheads indicate doubly stained cells. Adapted from Tse and Engler, 2011.

Figure 13| Quantification of β -III-tubulin (grey) and MyoD (black) by MSCs fluorescent intensity on gradient hydrogels (from 1 to 11 kPa, filled squares) and normalized to the non-permissive static hydrogels (1 and 11 kPa each and only, open circles). Adapted from Tse and Engler, 2011.

Figure 14| Represent the results of gene (CD73, CD90 and CD105) expression for 7 days (D7) and 14 days (D14) in the Col-HA scaffolds of EDC 0.1% and EDC 2.0% which have stiffnesses of approximately 1 and 10 kPa, respectively, and were defined as soft and stiff substrates, respectively. The results were compared to individual day 1 gene expression levels. Adapted from Her et al., 2013).

Figure 15| Representative images of phase-contrast microscopy of cells cultured on ≈ 7 kPa PA hydrogels in which small spots of $2.5 \pm 0.5 \text{ mm}^2$ had been previously functionalized with different COL-1 concentrations (as indicated) to assess cell adhesion 1 and 6 days after seeding. MSCs were plated at 3000 cells/cm^2 ($n=2$). Bar represents 100 μm .

Figure 16| Left and right upper images: Representative fluorescence microscopy images of hMSCs plated on polyacrylamide hydrogels with 12.5% acrylamide at day 1 (left) and 5 (right) after being fixed and stained with DAPI (in blue). Size bar corresponds to 200 μm . Bottom graphic: Proliferation assay of hMSCs in polyacrylamide hydrogels, showing the fold increase of the number of cells from day 1 to day 5 ($n=3$).

Figure 17| Colonies of hMSCs isolated in different PA hydrogels from UCM-WJ fragments after 1 week and 2 weeks of fragments plating in the hydrogels with just COL-1 or with COL-1 and FN (n=2). Bar corresponds to 200µm.

Figure 18| Immunophenotype of UCM-MSCs. The Y axis is the cell density. The X axis is a logarithmic scale of fluorescence. Cells were detached, labelled with antibodies against the indicated antigens and analyzed by flow cytometry. Cells were positive for CD49e, CD73, CD13 and CD90 (red and green lines) when compared with unlabeled MSCs (dark gray and light gray) for the 2 conditions, both from the PA hydrogels and the Plastic/TCPs (n=1).

Figure 19| Immunophenotype of UCM-MSCs. The Y axis is the cell density. The X axis is a logarithmic scale of fluorescence. Cells were detached, labelled with antibodies against the indicated antigens and analyzed by flow cytometry. Cells were negative for CD11b, HLA-DR, CD45 (red and green lines) when compared with unlabelled MSCs (dark gray and light gray) for the 2 conditions, both from the hydrogels and of the Plastic/TCPs (n=1).

Figure 20| hMSCs cultured on TCPs (Plastic) and PA hydrogels coated with COL-1 for 7 days after being treated with mitomycin C to inhibit proliferation. Cells were stained with anti-B-III tubulin (red), anti-Nestin antibodies (green) and DAPI (blue). This experiment was performed once (n=1). Bar corresponds to 400µm.

Figure 21| hMSCs cultured on TCPs (Plastic) and PA hydrogels coated with COL-1 for 7 days after being treated with mitomycin C to inhibit proliferation. Cells were stained with anti-GFAP (red), anti-O4 antibodies (green) and DAPI (blue). This experiment was performed once (n=1). Bar corresponds to 400µm.

Figure 22| hMSCs cultured on TCP (Plastic) and PA hydrogels coated with COL-1 for 7 days after being treated with mitomycin C to inhibit proliferation. Cells on the 7kPa hydrogels and 1kPa hydrogels were isolated on 12 kPa hydrogels as mentioned in III.4.

Cells were stained with anti-B-III tubulin (red), anti-Nestin antibodies (green) and DAPI (blue). This experiment was performed once (n=1). Bar corresponds to 200 μ m.

Figure 23| hMSCs cultured on TCP (Plastic) and PA hydrogels coated with COL-1 for 7 days after being treated with mitomycin C to inhibit proliferation, the cells on the 7kPa hydrogels and 1kPa hydrogels were isolated on 12 kPa hydrogels as mentioned in III.4. Cells were stained with anti-GFAP (red), anti-O4 antibodies (green) and DAPI (blue). This experiment was performed once (n=1) for GFAP and twice for O4 (n=2). Bar corresponds to 200 μ m.

List of tables

Table I - Composition of the hydrogels solutions - volume added of each reagent (μL) per one milliliter of solution.

Table II - Mean \pm standard deviation (SD) of the Young's modulus (E) (amount of force per unit of area needed to deform the material by a given fractional amount without any permanent deformation) calculated from the shear modulus measured at 1Hz, according to the formula $E = 2G'(1+\nu)$, where G' is the shear storage modulus measured by the rheometer and ν is the Poisson ratio, assumed to be 0.5 (Moore 2010). Values represent results of measurement of three independent hydrogels (n=3).

* Hydrogels previously characterized in the laboratory (Lourenço, 2012).

Table III - Mean, Median and Coefficient of variation of the Fluorescence values obtained by flow cytometry for the positive MSCs markers (CD49e, CD73, CD13 and CD90) for cells isolated and cultured on PA hydrogels and from TCPs (n=1).

List of abbreviations

AA	- Acetic Acid
Ac	- Acrylamide
AJ	- Adherens junctions
ALP	- Alkaline phosphatase
Bac	- Bisacrylamide
BM	- Bone marrow
CD	- Cluster of differentiation
COL-1	- Collagen type 1
CFU-F	- Colony-forming unit-fibroblast
DAPI	- 4',6-Diamidino-2-phenylindole dihydrochloride
Desm	- Desmosomes
E	- Elastic modulus
ECM	- Extra-cellular matrix
ESC	- Embryonic stem cell
FA	- Focal adhesion
FAK	- Focal adhesion kinase
FRET	- Forster Resonance Energy Transfer
FN	- Fibronectin
FX	- Focal complex
GAP	- GAP junctions
GFAP	- Glial fibrillary acidic protein
GR	- Growth factor receptor
HLA-DR	- Human leucocyte antigens disease resistant
hMSC	- Human mesenchymal stem cell
kPa	- Kilopascal
Lip	- Lipid droplets
MAP2	- Microtubule-associated protein 2
ML	- Myosin light chain kinase

MSC	- Mesenchymal stem cell
N	- Nestin
n	- Number of experiments done
NA	- Nascent adhesions
Ns	- Nesprins
NSC	- Neural stem cell
NF-H	- Neurofilament, Heavy Chain
ISCT	-International Society of Cellular Therapy
PA	- Polyacrylamide
Pa	- Pascal
Pax	- Paxillin
PM	- Proliferation Medium
qPCR	- quantitative reverse transcriptase-polymerase chain reaction
SD	- Standard deviation
TRP	- Transient receptor potential
TMED	- Tetramethylethylenediamine
TCPs	- Tissue-culture polystyrene
TCP	- Tissue culture plate
UC	- Umbilical Cord
UCB	- Umbilical cord blood
UCF	- Umbilical Cord Fragment
UCM	- Umbilical Cord Matrix
WJ	- Wharton's jelly
V	- Poisson ratio

Chapter I

Introduction

I - Introduction

I.1 - Mesenchymal stem cells (MSCs)

Mesenchymal stem cells (MSCs), also referred to as mesenchymal stromal cells or mesenchymal progenitor cells were identified for the first time in the bone marrow (BM) and were described as a population of plastic-adherent, non-hematopoietic and spindle-shaped mesenchymal precursor cells. Due to their ability to form colonies of cells similar to fibroblasts, those colonies were called, colony-forming unit-fibroblast (CFU-Fs) (Friedenstein et al., 1970). As the studies and years advanced, observations over MSCs showed that those cells from the bone marrow were multipotent and could differentiate into osteoblasts, chondroblasts, myoblasts and adipocytes (Prockop, 1997; Nardi and da Silva Meirelles, 2006).

Therefore, MSCs are currently defined as multipotent cells capable of self-renewal that can differentiate into different mesenchymal cell phenotypes (da Silva Meirelles et al., 2008).

I.1.1 - Sources of MSCs

Although MSCs were initially identified and characterized in the bone marrow (BM), with the years and research they have also been isolated from adipose and other human adult tissues (Friedenstein et al., 1974; Zuk et al., 2001).

As there is a great interest for cells with proliferation and differentiation potential and also because in adult tissues with ageing there is a decrease of MSCs frequency and their differentiation capacity, alternative sources have been explored. In this way, MSCs have been identified in several fetal tissues (including BM, liver, blood, lung and spleen) but their full potential for use in clinical trials has been compromised by technical and ethical factors (Malgieri et al., 2010). Hence, alternatives like other primitive sources, namely extra-embryonic tissues like the umbilical cord blood (UCB), the umbilical cord matrix/Wharton's jelly (UCM/WJ), placenta and amniotic membrane have been studied and protocols for the extraction of MSCs from those tissues have been developed.

There are many advantages in using UCM as an alternative source of human MSCs when comparing to BM and other adult tissues. Because the umbilical cord (UC) physiologically supports development of the embryo only throughout fetal life until birth, it is normally discarded at birth, being a tremendous waste, since the procedure of collection is painless, non-invasive and harmless either to the mother or the newborn. This procedure can increase the potential donors of MSCs (Weiss and Troyer 2006) and diminish the ethical and clinical issues (Malgieri et al., 2010). Moreover, those are not the only positive aspects, there is also the fact that MSCs isolated from the UC seem to be more primitive, have greater expansion capacity *in vitro* and shorter doubling time than MSCs isolated from adult tissues (Park et al., 2006). Despite not being as immature as embryonic stem cells (ESCs), UCM- and UCB-MSCs have a big differentiation potential, being able to differentiate into cell types with characteristics of the three germ layers and with very low chances to develop tumors when transplanted (Lee et al., 2004).

When comparing the efficiency of MSCs isolation from the UC tissues (blood and matrix), the blood is the one with lower efficiency (about 30%) (Bieback et al., 2004) and this is a disadvantage when compared with the matrix that has been consistently reported as having an efficiency of 100% (Secco et al., 2008; Zeddou et al., 2010; Taghizadeh et al., 2011).

1.1.2 - *In vitro* characterization of MSCs

For many years the search for the identity of mesenchymal stem cell was mainly dependent on three culture systems: the CFU-F assay, the isolation and analysis of bone marrow stroma, and the cultivation of mesenchymal stem cell lines. The isolation and culture conditions used to expand these cells rely mostly on the ability of MSCs to adhere to plastic surfaces. MSCs populations in culture are typically composed by cells that comprise some heterogeneity, in terms of differentiation potential and expression of secondary MSC markers. Whether the culture conditions selectively favor the expansion of different bone marrow precursors or induce similar cell populations to acquire different phenotypes is not clear (Nardi and da Silva Meirelles, 2006).

I.1.2.1 - Immunophenotype

The Mesenchymal and Tissue Stem Cell Committee of the International Society for Cellular Therapy proposed 3 minimal criteria to define human MSCs. Those are: i) MSCs must be plastic-adherent when maintained in standard culture conditions; ii) MSCs must express CD105, CD73 and CD90, and lack expression of CD45, CD34, CD14 or CD11b, CD79a or CD19 and HLA-DR surface molecules; iii) MSCs must differentiate to osteoblasts, adipocytes and chondroblasts *in vitro* (Dominici et al., 2006). Although MSCs express a high number of cell surface markers and those were all well characterized, there is still no specific marker identified. However, there is a typical neuroectodermal marker, nestin, which began to be regarded as a good marker for the identification of MSCs (Mendez-Ferrer et al., 2010) and seems to be in agreement with reports indicating at least a partial neuroectodermal origin of MSCs (Takashima et al., 2007; Morikawa et al., 2009).

I.1.2.2 - CFU-F and proliferation capacity

Colony formation capacity is an important hallmark of stem cells and it demonstrates the presence of highly proliferative cells in these cultures (Javazon et al., 2001). MSCs also have the ability to form colonies *in vitro* after low-density plating or single-cell sorting, however colonies derived from those assays are heterogeneous in morphology, size and differentiation potential (Owen and Friedenstein, 1988; Kuznetsov et al., 1997; Dominici et al., 2006).

I.1.2.3 - Multilineage differentiation capacity

MSCs are multipotent progenitor cells with the capability to differentiate *in vivo* and *in vitro* into adipogenic, chondrogenic and osteogenic lineages (Caplan, 2009). This capacity to differentiate *in vitro* into several mesenchymal phenotypes was what in 2006 the ISCT had defined as one of the main properties integrating the minimal criteria that define MSCs (Dominici et al., 2006). However, those lineages are not the

only ones MSCs can differentiate into. It has been shown that the differentiation potential of these cells covers cells with markers characteristic of the three germ layers (ectoderm, mesoderm and endoderm), like cells similar to cardiomyocytes (Wang et al., 2004), skeletal muscle cells (Conconi et al., 2006), endothelial cells (Wu et al., 2007), hepatocytes (Lee et al., 2004; Anzalone et al., 2010) and neural-like lineages (Weiss et al., 2003; Sanchez-Ramos et al., 2008).

Of particular interest for this thesis, is the neural-like differentiation of MSCs. It was demonstrated that nestin-positive MSCs can differentiate into neuron-like cells (Wislet-Gendebien et al., 2005) and probably the expression of this neuroectodermal marker is related with the neuroepithelial origin of these cells (Takashima et al., 2007; Mendez-Ferrer et al., 2010). Further studies also showed that nestin-positive MSCs were induced to a neural stem-like cell fate and then converted into oligodendrocyte precursor-like cells (Zhang et al., 2010), reinforcing the idea that nestin-positive MSCs have the capability to differentiate into neural-like lineages.

1.2. - Mechanotransduction and its implications in cellular fate

Mechanical forces are normally implicated in the regulation of many physiologic and pathologic processes and are the basis of mechanotransduction. Mechanical loading can induce hypertrophy and strengthening of muscles, tendons, ligaments and bones, whereas prolonged exposure to weightlessness seems to make the opposite, e.g. left early astronauts prone to bone fractures (Burkholder, 2007; Duncan and Turner, 1995; Hattner and McMillan, 1968). Similar hypertrophic thickening, but this time due to pathogenic symptoms, occurs in the heart with unchecked hypertension, although in this case potentially dangerous consequences may occur (Weber et al., 1989; Westerhof and O'Rourke, 1995). Differences in the flow-induced shear stress on veins or arteries specify their endothelium differentiation in part to become a venous or arterial phenotype, and certain regions are more susceptible to inflammation due to the distribution of shear stresses within the arterial tree, explaining the observed distribution of atherosclerotic plaques (Davies et al., 1995; Garcia-Cardena et al., 2001). The contractile activity of cells generates mechanical forces that drive physical changes in a developing embryo, but also are

transduced to affect cellular signaling, gene expression and cell function, which are crucial to developmental programming (Lee et al., 2006; Somogyi and Rorth, 2004; Farge, 2003). (Ingber et al., 1986a; Ingber and Folkman, 1989b). It was shown that changes in the balance of mechanical forces between integrins and cytoskeleton that accompany cells spreading and drive cytoskeletal restructuring control downstream mitogenic signaling cascades and thereby control the cellular response to other external stimuli. So mechanical forces are equally important biological regulators as growth factors and ECM are (Huang et al., 1998).

It has long been noted that the differentiation of stem cells into multiple lineages is accompanied by dramatic changes in cell morphologies, and the demonstration that mechanical cues influence lineage commitment of stem cells (McBeath et al., 2004). So, inhibition of cell-generated forces was showed to alter many basic cellular functions, such as proliferation, differentiation, tissue organization and migration (Huang et al., 1998; McBeath et al., 2004; Sordella et al., 2003; Krieg et al., 2008; Lo et al., 2004).

By modulating the stress that is generated by these cellular forces altering the mechanical stiffness of the substrate it is possible to achieve a similar response to the one caused by directly altering cellular contractility (Pelham and Wang, 1997; Paszek and Weaver, 2004; Engler et al., 2006).

Stiffness is the extent to which a substrate resists deformation. Substrate stiffness itself can alter numerous cellular functions including migration, proliferation and differentiation (Li et al., 2007; Peyton and Putnam, 2005; Leach et al., 2007; Lo et al., 2000).

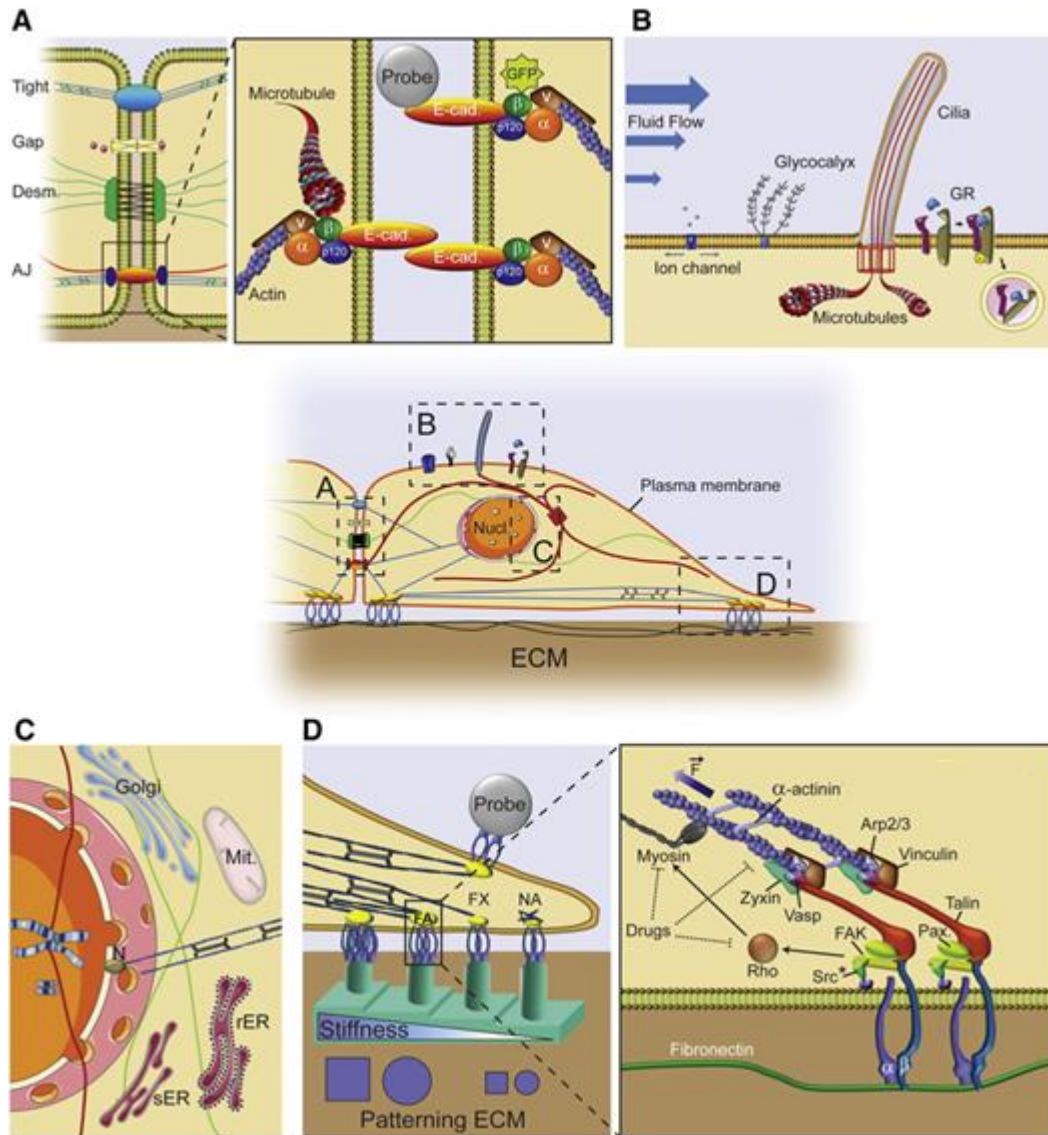


Figure 1. Mechanotransduction in a Cell-ECM Unit: Center image – A cell connected to another cell and to the ECM. Center image (A) and (D)- show where mechanotransduction in the cell-ECM unit occurs. The “blue lines” represent actomyosin filaments, “green lines” embody intermediate filaments and the “red lines” correspond to microtubules in all panels. Integrins are represented by the “blue structures” linking the cell with the ECM (D); Center “nucl.” – nucleus; (A)-Mechanotransduction at adherens junctions; (A, LEFT) Shows different cell-cell junctions –“Tight” is for tight junctions. “GAP” is for Gap junctions. “Desm” is for desmosomes. “AJ” is for Adherens junctions. (A, RIGHT): Shows the Molecular structure of an AJ: E-cad: E-Cadherin, a: Alpha Catenin, b: Beta Catenin, p120: p120 Catenin, v: Vinculin; (B)-Mechanoreceptors at the cell membrane. Deformation of the plasma membrane by the fluid flow or stretching, leads to activation of ion channels resulting in an ions influx. Furthermore fluid flow directly impacts glyocalyx and cilia movement which triggers diverse downstream signaling cascades. Mechanical forces also mediate growth factor receptor (GR) clustering and endocytosis, and thus affect GR signal transduction as well; (C) - Mechanotransduction at the nucleus. Intermediate filaments and microtubules are interconnected with the nucleus and surrounding organelles (Golgi apparatus, Mitochondria, rough and smooth endoplasmic reticulum). Nesprins (Ns) bind the nucleus with the actomyosin cytoskeleton. With the change in cell shape and contractility there is an alteration to spatial localization of organelles which may lead to a conformational change in the nuclear pores. (D) - Mechanotransduction at the focal adhesion (FA). (D, LEFT): Nascent adhesions (NA), focal complexes

(FXs) and focal adhesions (FA), undergo through a maturing process controlled by actomyosin contractility which can be modified by stiffness, shape or external application of force. (*D, RIGHT*): molecular structure of FA. α/β : alpha and beta sub-units of integrins, Pax: paxillin, F: Force delivered by actomyosin contraction. The clustering of integrins may induce RhoA signaling which leads to an increase of myosin contractility and an unfolding of proteins. Adapted from Eyckmans et al., 2011.

I.2.1 - Mechanotransduction and mechanosensors

Generation of forces on the matrix can be sensed through integrins by 5 basic mechanisms that have been suggested for mechano-sensing: catch bond formation, channel opening, enzyme regulation, exposure of phosphorylation sites, or exposure of binding sites. All could play significant roles in adhesion-related processes (Moore et al., 2010).

Looking over mechanotransduction more closely, it is known that changes in cell shape and cytoskeletal architecture are related with the integrins binding and clustering against ECM ligands, anchoring the actin cytoskeleton to sites of adhesion.

The orientation of the integrin layer within the cell membrane is made with the head domains connecting to the ECM and the cytoplasmic tails binding to focal adhesion kinase (FAK) and paxillin. This cytoplasmatic layer is assembled with complexes containing talin and vinculin, and an uppermost actin-regulatory sheet consisting of zyxin, VASP and α -actinin that binds the cytoskeleton to the FA (Figure 1D) (Kanchanawong et al., 2010).

Since the cytoskeleton is linked to the nuclear envelope, forces experienced or generated by the cell-ECM module (Figure 1) are transmitted and sensed throughout as a coordinated system (Eyckmans et al., 2011). The actomyosin cytoskeleton works as a connection between multiple parts of the cell membrane as well as the cell membrane to the nucleus (Sims et al., 1992). These filaments anchor into clusters of proteins (including focal adhesions, FAs) which link the ECM to the cytoskeleton through transmembrane integrin receptors (Eyckmans et al., 2011). So if there is application of a force to the cell-ECM unit, structural deformations and rearrangements of the ECM will occur, the force is transmitted through the FA, and almost every single aspect of the intracellular structure, like the position of endoplasmic reticulum, mitochondria and the nucleus will get deformed (Figure

1C)(Dogterom et al., 2005). Not only intracellular structure gets deformed but also receptor-mediated transduction of forces have been convincingly shown for integrins (Wang et al., 1993) and stretch-activated ion channels (Lansman et al., 1987; Sadoshima et al., 1992). Mechanical forces, for stretch-activated receptors, appears to alter the conformation of the Transient Receptor Potential (TRP) family of channels, leading to rapid signaling responses (such as calcium influx, <4 ms) following mechanical perturbations (Figure 1B) (Matthews et al., 2010).

In vivo, cells are generally tightly connected to each other via cell-cell junctions (Figure 1A) and adherens junctions (AJ) link the cytoskeletons of adjacent cells via clusters of cadherins (Yamada et al., 2005).

Manipulation of Cell-ECM forces can be done by using traditional molecular methods to directly target the force-generating mechanism and apparatus. A wide amount of pharmacological inhibitors that behave like modulators of contractility are available and able to act in several related mechanisms/proteins like the molecular motor myosin II (blebbistatin), the upstream regulators of myosin phosphorylation Myosin Light Chain Kinase (ML-6, ML-9), and the Rho/ ROCK signaling pathway (fasudil, Y27639, C3 botulinum exotoxin), as well as the polymerization processes of actin (latrunculin, cytochalasin D), (Figure 1D) (Eyckmans et al., 2011).

It is thought that at least in part, the effects of ECM stiffness on cells are similar to effects of decreased integrin-mediated adhesion and cellular force generation. And this is because cells can transduce alterations due to substrate stiffness (even if the mechanism by which cells can do it is not fully understood) and it has been shown that cells attached to more compliant substrates exhibit immature FAs, decreased traction force generation, and suppressed integrin activation. When using hydrogels it can also occur alterations in the internal structure, growth factor adhesion and surface topology of the hydrogels due to the crosslinking chemistry (Houseman and Mrksich, 2001; Keselowsky et al., 2005; Crouzier et al., 2011).

Cilia and primary cilia also have a role in mechanotransduction studies. They are microtubule-based structures enveloped in a specialized membrane that originate from the cell body into the extracellular space and that take part in the development of organs and tissues, such as kidney, pancreas, liver, cartilage, and bone among others (Figure 1B). Although the molecular basis for cilia mechanosensing is still not

completely understood, they seem to transduce mechanical stimuli by modulating Wnt and Sonic Hedgehog signaling or/ and gating polycystin-based ion channels (Wallingford, 2010; Wallingford and Mitchell, 2011; Bisgrove and Yost, 2006; Berbari et al., 2009).

I.2.2 - Extracellular matrix and integrin-based mechanotransduction mechanisms

The extracellular matrix (ECM) mediates changes in cell shape according to its mechanical properties and most adherent cells have a very their own shape but non-adherent cell types are usually rounded and change shape when they attach to surrounding tissue (Discher et al., 2009), suggesting that adherent cells can sense and respond to mechanical signals from the ECM. The regulated interplay of intracellular contractile forces and extracellular attachment might determine cellular shapes (Bauer et al., 2009). Focal adhesions and other membrane sensors (e.g. tight junctions and primary cilia) alter their structure and function as a result of changes in mechanical stress when cells are attached to substrates of different stiffness (Chen et al., 2008).

Changes in stiffness can cause a change in cell shape and it is observed that cells retain a more rounded morphology on soft substrates and take on a more flattened shape on stiff substrates (normally associated with cells cultured on hard tissue culture polystyrene) (Chen et al., 2008).

I.2.2.1 - Mechanisms of Rigidity Sensing

Substrate rigidity, besides changing cell shape can also influence a number of cellular processes including retraction forces, cell adhesion, actin flow, gene expression, and cell lineage (Bard and Hay, 1975; Choquet et al., 1997; Engler et al., 2006; Lo et al., 2000; Pelham and Wang, 1997; Peyton and Putnam, 2005). The nature of the matrix and the cell-type specific components involved in the responses will define the rigidity responses. However, in a basic way, integrin-mediated rigidity sensing can be taken as the decision to couple and reinforce the link between an

extracellular ligand and the cytoskeleton. So whether integrin-cytoskeleton bonds become reinforced depends upon the intracellular component and the mechanical properties of the microenvironment that make up this link.

The activation of Src family kinases is involved in the ligand binding to integrins. This is supported because when applied a force, Src family have a rapid activation (within 300 ms) and was observed that Src family kinases Fyn and Src are required for rigidity sensing on fibronectin and vitronectin, respectively (Felsenfeld et al., 1999; Kostic and Sheetz, 2006; Na et al., 2008). The activation of the Src family kinases will bridge integrins to the cytoskeleton through talin (Duband et al., 1988; Felsenfeld et al., 1996; Schmidt et al., 1993; Zhang et al., 2008). Ligand binding couples integrins to the cytoskeleton once coupled to retrograde flowing actin, mechanical force on integrins could engage the integrin/ECM catch bond. Under stretching forces, Talin exposes vinculin binding sites (Figure 2C) that stabilize and recruit additional links to actin (del Rio et al., 2009). To restart the process the activation of FAK may reverse adhesions (Ilic et al., 1995; Zhang et al., 2008).

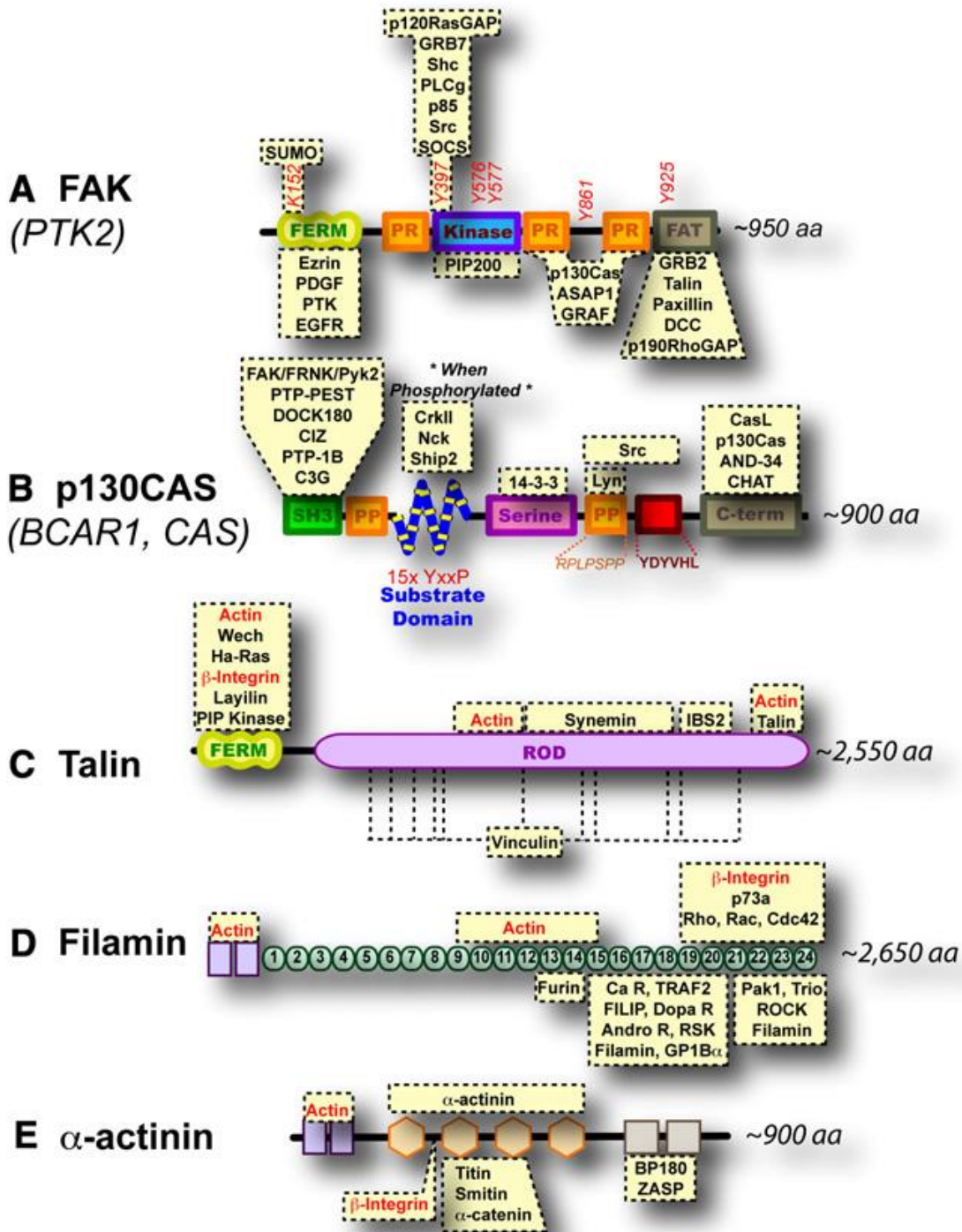


Figure 2 - Proteins related to the mechanosensory in Integrin-Mediated Rigidity Sensing. The yellow boxes highlight the proteins which bind directly to the depicted domains. (A) FAK activity is regulated by mechanical force but does not bind integrins or actin directly. (B) Stretching the p130Cas domain exposes its 15 tyrosine residues. (C) Stretching of talin's rod domain exposes vinculin binding sites (del Rio et al., 2009). (D) Extension of filamin immunoglobulin repeats (labeled 1–24) has been shown by AFM (Furuike et al., 2001) and could regulate the binding of proteins. (E) α -actinin forms antiparallel dimers; mechanical force could regulate this dimerization or its association with other proteins. Adapted from Moore et al., 2010.

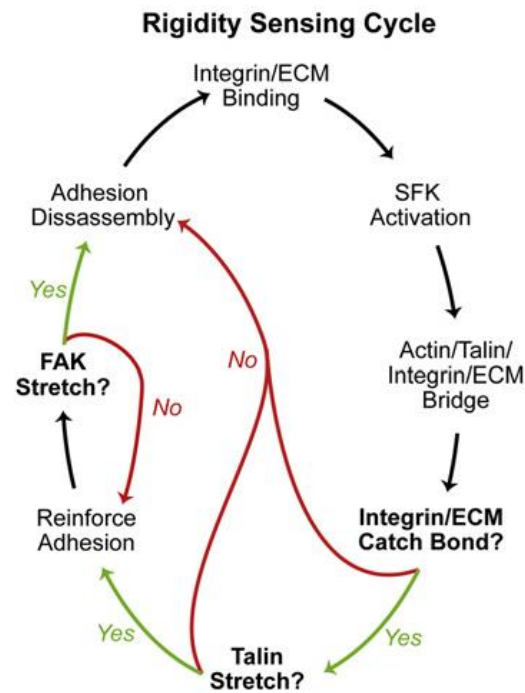


Figure 3 - The Rigidity Sensing Cycle. In this rigidity sensing cycle scheme it is shown the correlation between mechanosensory events as integrin/ECM catch bond formation, stretching of talin (that recruits vinculin and therefore reinforces the adhesion) and stretching of FAK, leading to the disassembly and recycling of the adhesion, by the activation of its kinase domain. Adapted from; Moore et al., 2010

This transient and multiple steps active process of rigidity sensing is sensitive to the matrix rigidity (Figure 3) and so the cell retraction speed (loading rate) felt on the integrin-ECM catch bond is determined by the substrate rigidity. Just as catch bonds have a force providing maximum lifetime in a scenario of constant force application, they will have a corresponding optimal loading rate in scenarios where force is loaded progressively. But the loading rate, at the optimal rigidity, will maximize bond lifetime, triggering subsequent mechanotransduction events when a force is applied. Coupling between rearward flowing actin and the substrate is the key for rigidity sensing (Moore et al., 2010).

I.2.3 - Mechanotransduction and Stem Cells

I.2.3.1 - Mechanotransduction and MSCs differentiation

Living tissues are known to possess different physiologic characteristics according to their function and cellular type, so considering the elasticity of solid tissues, very different values of elasticity can be found as shown in Figure 4. The solid tissues exhibit a range of stiffness, as measured by the elastic modulus, E (Engler et al., 2006).



Figure 4 – Tissue Elasticity. Range of stiffness measured by the elastic modulus, E , of some human solid tissues. Adapted from Engler et al., 2006.

Mesenchymal stem cells will differentiate into different phenotypes as a function of substrate stiffness. The lineage they can differentiate into when cultured on a substrate with a certain range of stiffness has phenotypic features similar to cells found in the solid tissues with the same range of stiffness (Figure 4), and MSCs appear to do so in a way that would promote tissue-specific differentiation and healing (Engler et al., 2006). For example, on brain-tissue-like stiffness cells undergo neuronal-like differentiation, whereas muscle-equivalent stiffness promotes myogenesis (Figure 5) (Engler et al., 2006).

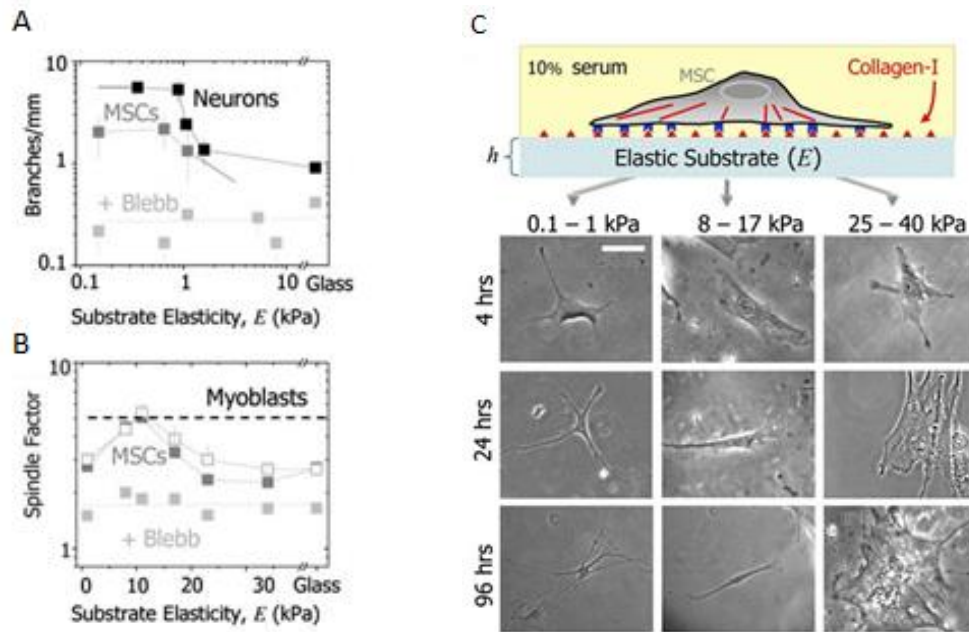


Figure 5 - Images depicted on A) and B) quantify the morphological changes (mean \pm SEM) versus stiffness, E : shown are (A) cell branching per length of primary mouse neurons, MSCs, and blebbistatin-treated MSCs and (B) spindle morphology of MSCs, blebbistatin-treated MSCs, and mitomycin-C treated MSCs (open squares) compared to C2C12 myoblasts (dashed line). Furthermore in C) MSCs change their morphology developing increasingly branched, spindle, or polygonal shapes, respectively, when cultured on matrices with the elastic modulus (E) respectively in the range typical of brain (0.1–1 kPa), muscle (8–17 kPa), or stiff crosslinked-collagen matrices (25–40 kPa). Blebbistatin blocks morphology changes due to stiffness (<2-fold different from naive MSCs) and mitomycin-C inhibit cell proliferation. Adapted from Engler et al., 2006.

Analyzing the cells morphologies of Figure 5C, we can see that matrix-dependent shape variations of MSCs are similar to primary neurons. Furthermore, since the inhibition of proliferation by mitomycin-C (open squares, Figure 5 A) has little impact on average cell shape, the morphology results are consistent with lineage development being a population-level response to substrate elasticity (Engler et al., 2006).

Transcriptional profiles of neurogenic, myogenic, and osteogenic markers (from early commitment markers through mid/late development markers) (Figure 6) support the morphology indications (Figure 5 A and B). This means that, as expected from the softest gels, MSCs showed the greatest expression of neurogenic transcripts (Figure 6) because the neuron-specific cytoskeletal markers are all upregulated (Engler et al.,

2006), such as nestin, an early commitment marker, and Beta-III tubulin, expressed in neurons, as well as the mature marker neurofilament light chain (NFL) (Lariviere and Julien, 2004) and the early/mid adhesion protein NCAM (Rutishauser, 1984). RNA profiles indicate lineage specification on matrices of tissue-like stiffness.

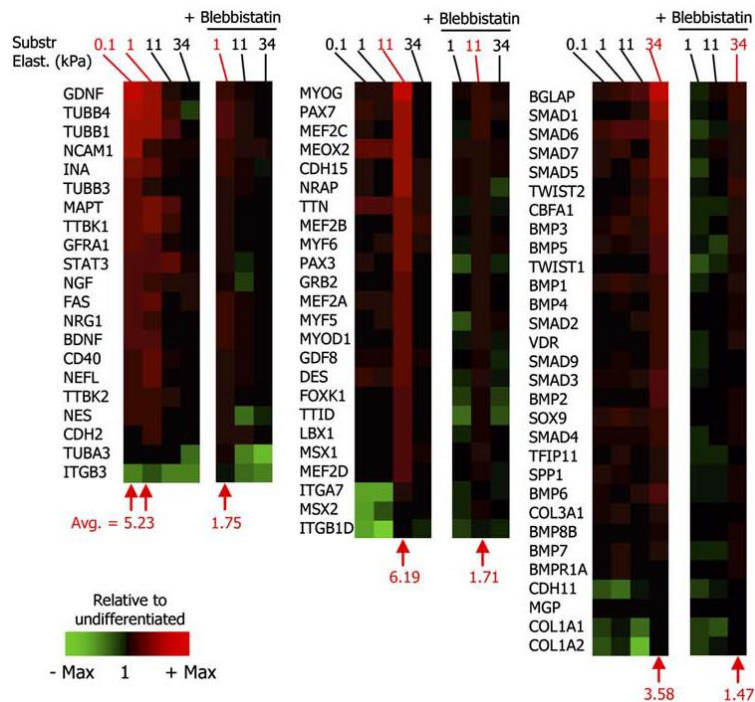


Figure 6 - Microarray profiling of MSC transcripts in cells cultured on 0.1, 1, 11, or 34 kPa matrices with or without blebbistatin treatment. Results are normalized to actin levels and then normalized again to expression in naive MSCs, yielding the fold increase at the bottom of each array. Neurogenic markers (left) are clearly highest on 0.1–1 kPa gels, while myogenic markers (center) are highest on 11 kPa gels and osteogenic markers (right) are highest on 34 kPa gels. Adapted from Engler et al., 2006).

To clarify neuro-induction microenvironments and the time series of images in Figure 5 that shows outwardly branching MSCs on the softest gels (0.1–1 kPa) it was seen that, in immunofluorescence (Figure 7 A), also show expression and branch localization of neuron-specific Beta-III tubulin and neurofilament heavy chain (NFH and its phosphoform, P-NFH) (Engler et al., 2006).

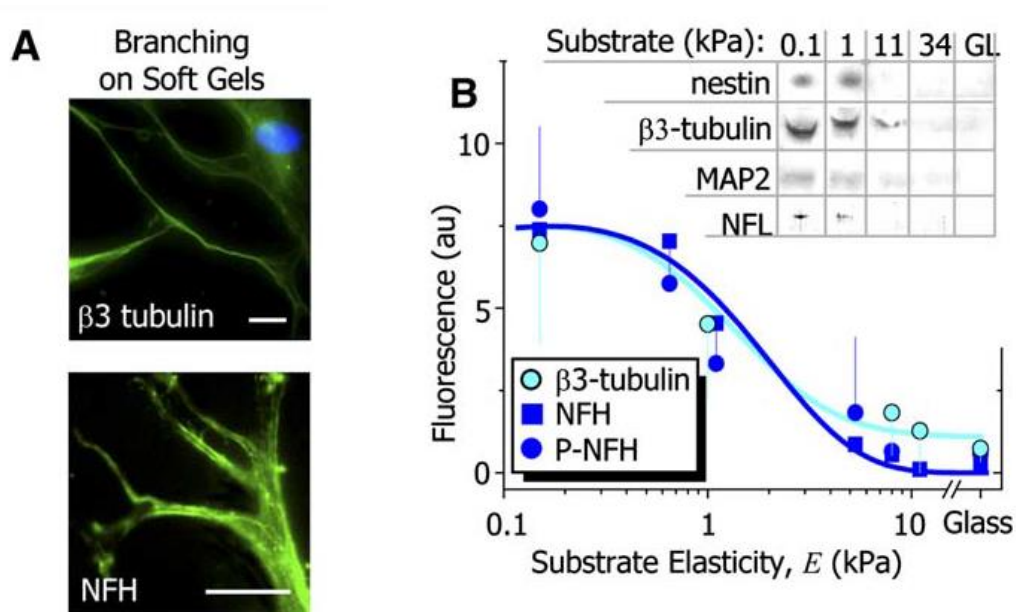


Figure 7 - A) Immunofluorescence images of Beta-III tubulin and NFH in branched extensions of MSCs on soft matrices ($E \approx 1$ kPa). Scale bars are 5 mm. B) B-III tubulin, NFH, and P-NFH all localize to the branches of MSCs on the softest substrates with $E < 1$ kPa (mean \pm SEM). Nestin, B-III tubulin, MAP2, and NFL Western blotting (inset) confirms expression only on soft gels (GL = Glass). Adapted from Engler et al., 2006.

Intensity analyses of immunofluorescence images as well as Western blots (Figure 7) confirm that proteins markers for neural commitment are expressed only in cells on the softest matrices. Protein markers for neuronal commitment (nestin), immature neurons (B-III tubulin), mid/late neurons (microtubule associated protein 2; MAP2), and even mature neurons (NFL, NFH, and P-NFH) (Engler et al., 2006). These results from Engler et al. 2006 suggest that this process that occurs with MSCs somehow recapitulates what is seen during neurogenesis *in vivo*, as seen in more complex microenvironments like the brain (Kondo et al., 2005; Wislet-Gendebien et al., 2005).

Furthermore, when looking across the range of matrix stiffness, to the cytoskeletal markers and transcription factors characteristic of the distinct lineages (Figure 8) it is indicated that MSCs lineage specification occurs (process similar to an incomplete differentiation), being consistent with the lineage profiling of Figure 5 and 6. On the softest, neurogenic matrices, a majority of cells express B-III tubulin, which, along with P-NFH and NFH, is visible in long, branched extensions but is poorly expressed, if at all, in cells on stiffer gels (Figure 7). On moderately stiff, myogenic matrices, MSCs upregulate the transcription factor MyoD1, localizing it to the nucleus (Figure 8) (Engler et al., 2006).

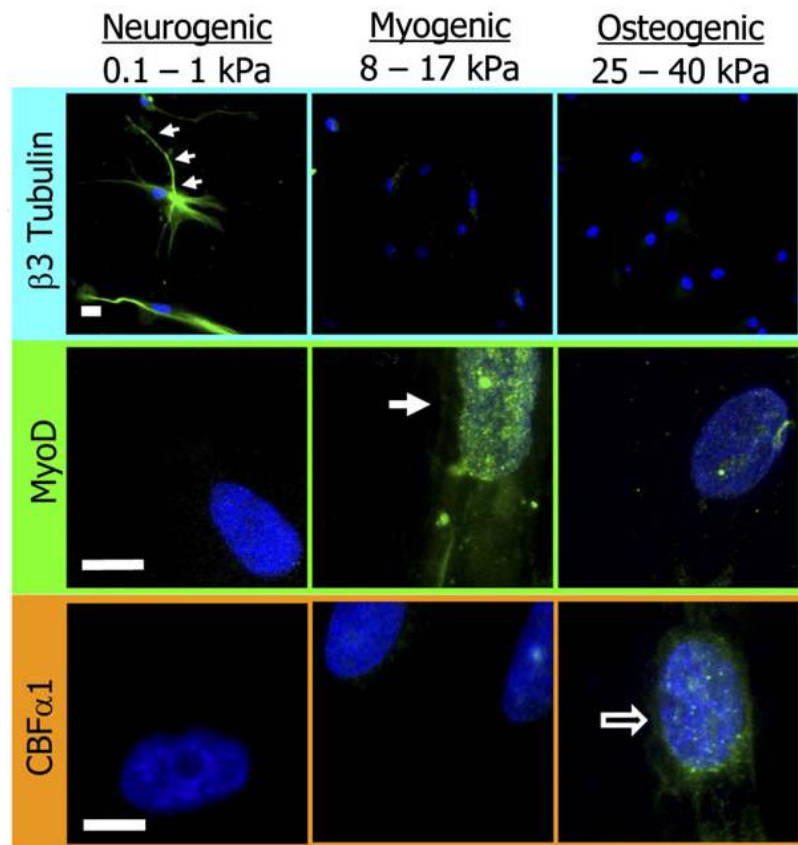


Figure 8 – Protein profile dependent of elasticity. The neuronal cytoskeletal marker (small arrows) B-III tubulin, the muscle transcription factor MyoD1 (filled arrow) and the osteoblast transcription factor CBF α 1 (empty arrow) are only expressed on the soft, myogenic and stiff matrices respectively. Scale bar is 5 μ m. Adapted from Engler et al., 2006.

1.2.3.1.1 - Stiffness effect on Neuronal and Glial differentiation

The stiffness stimulus is very specific, being capable to induce lineage specifications on MSCs between glial- and neuronal-like lineages. As described by Her et al., 2013, human mesenchymal stem cells (hMSCs) in different 3-D Collagen–Hyaluronic Acid scaffolds can express specific markers for glial and neuronal lineages between the stiffness range of \approx 1 and \approx 10 kPa. They studied the following neural lineage specific genes: Nestin [gene marker of neural stem cells (NSCs)]; SOX2 (developmental gene marker of the neural lineage); B-III tubulin (is a common neuronal early marker which is a unique microtubule subunit that is found expressed almost exclusively in neurons) (Katsetos et al., 2003); Glial fibrillary acidic protein

(GFAP) (is a class-III intermediate filament which is the main constituent of intermediate filaments in astrocytes and it serves as a cell specific marker that distinguishes differentiated astrocytes from other glial cells during the development of the central nervous system)(Eng et al., 2000); CNPase (is a myelin-associated enzyme that makes up 4% of total central nervous system myelin protein and it is expressed exclusively by oligodendrocytes and Schwann cells) (Scherer et al., 1994); MAP2 (encodes a protein that belongs to the microtubule-associated protein family which is thought to be involved in microtubule assembly, it is an essential step in neurogenesis and is commonly recognized as a neuronal mid/late marker) (Dehmelt et al., 2004) and NF-H (for neuronal late marker, is a phosphorylated cytoskeletal intermediate filament protein expressed in neurons) (Black et al., 1988).

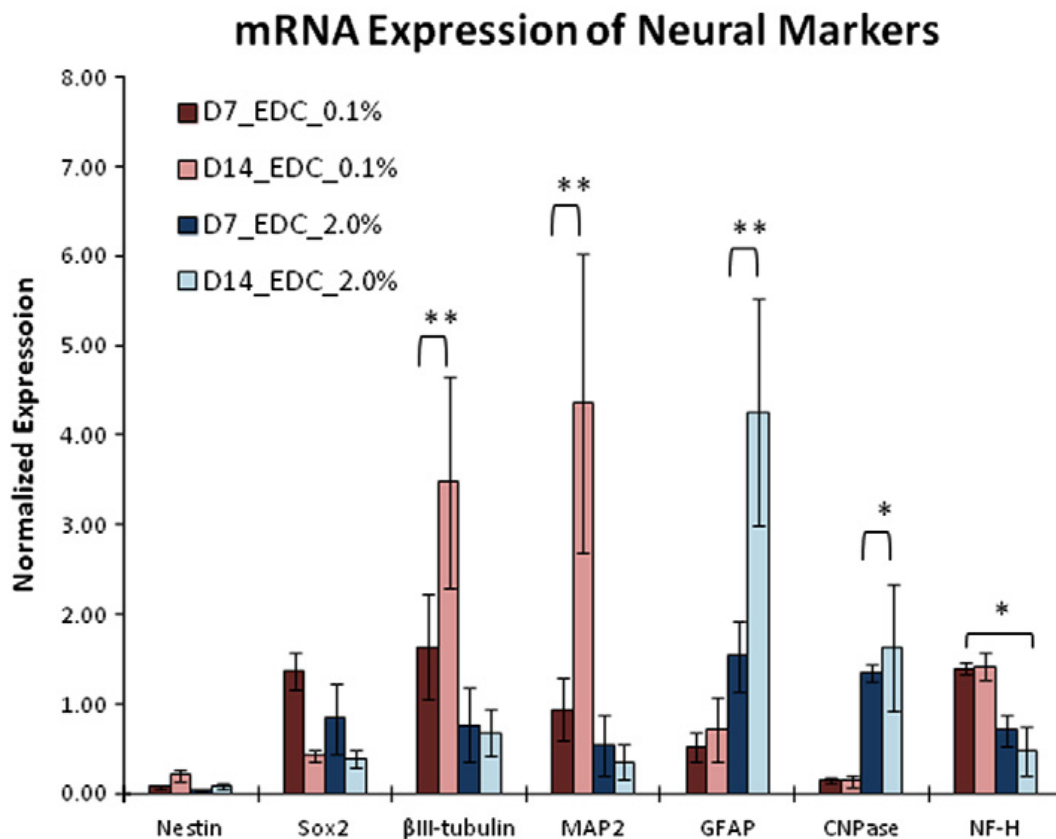


Figure 9 - Characterization of neural-like lineage differentiation of hMSCs in 3-D scaffolds. The graphic represents qRT-PCR results for representative neural lineage specific genes. D7= 7 days. D14 = 14 days. EDC_0.1% = \approx 1kPa. EDC_2.0% = \approx 10kPa (n =3, *P < 0.1, **P < 0.05) (Adapted from Her et al., 2013).

It was shown by quantitative reverse transcriptase-polymerase chain reaction (qRT-PCR) that nestin was found to be at relatively low levels indicating that the neural plasticity of hMSCs is different from the differentiation pathway of NSCs (Her et al., 2013). The neuronal lineage genes on soft substrate including β -III tubulin, MAP2 and NF-H were all obviously elevated in expression levels at days 7 and 14 when compared to that at day 1 ($E \approx 1$ kPa). This result was in agreement with that MSCs in soft substrate were likely to differentiate into neuronal-like cells (Engler et al., 2006). On the other hand, the glial lineage specific genes including GFAP and CNPase were dominantly expressed by hMSCs in stiffer substrates ($E \approx 10$ kPa) after 1 week in culture, indicating that MSCs in the 10 kPa substrate were likely to differentiate into glial-like cells. Of note was that the expressions of these genes including β III-tubulin and MAP2 in soft substrate and GFAP and CNPase in stiff substrate were all up-regulated at day 14 (Her et al., 2013).

In this study, both of the neuronal mid- and late- staged genes were dominantly up-regulated in the softer substrate after 1 week (Figure 9). MAP2 expression was significantly increased at 14 days while the NF-H expression was not so evident, suggesting that the differentiation of hMSCs toward neuronal lineage was a progressive process and hMSCs might require longer time to become fully matured neuronal-like cells (Her et al., 2013). So it is possible to induce differentiation of hMSCs towards neuronal- or glial-like lineages with just the stiffness stimulus.

1.2.3.2 - Manipulation and measurement of cellular forces in MSCs

There are different methods to test stiffness effects in mechanotransduction in the MSCs. Polyacrylamide hydrogels is one of the most utilized since it can have a surface with the elasticity that supports myogenic and osteogenic differentiation. The matrix elasticity is mimicked *in vitro* with inert polyacrylamide gels with concentrations of bis-acrylamide crosslinking that sets the desired elasticity (Pelham and Wang, 1997). Functionalizing the gels with collagen I provides adhesion points to cells (Engler et al., 2004a; Garcia and Reyes, 2005). Using a well-defined, elastic tunable gel system as opposed to wrinkling films or degrading collagen gels (Hinz et al., 2001; Wozniak et al., 2003), Engler et al. provided the first evidence with sparse cultures of MSCs that matrix

can specify lineage towards cells with characteristics of neurons, myoblasts, and osteoblasts.

Although hydrogels will continue to be important in characterizing and controlling cell-material interactions, other approaches can be used to better understand how cells sense changes in substrate rigidity.

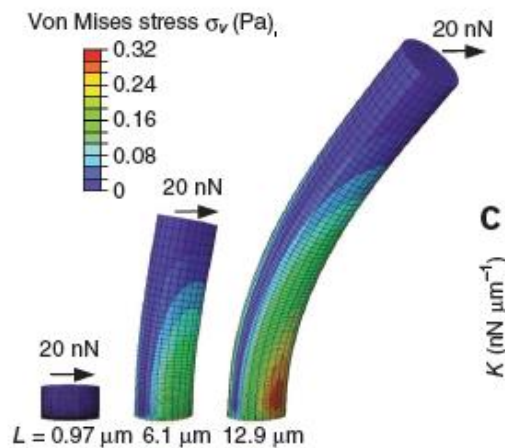


Figure 10 - Figure representing analysis of microposts heights (L) by finite-element method (FEM) each bending in response to applied horizontal traction force (F) of 20 nN. Adapted from Fu et al., 2010.

With the use of microposts we can also control substrate rigidity in which MSCs grow, different post heights control substrate rigidity, because microposts' height determines the degree to which a post bends in response to a horizontal traction force (Figure 10) (Fu et al., 2010).

On rigid (short) microposts, hMSCs were well spread with prominent, highly organized actin stress fibers and large focal adhesions. In contrast, cells on soft (long) microposts had a rounded morphology with prominent microvilli, disorganized actin filaments and small adhesion complexes (Fu et al., 2010).

Microposts can have advantages when compared with hydrogels because when checking for the rigidity sensing, it was demonstrated that rigidity sensing occurred at a micrometer scale, likely between focal adhesions because the nanoscale mechanics at the top of individual microposts (which could directly impact adhesion receptor binding) remain unchanged. Another advantage of micropost arrays over hydrogels was that measured subcellular traction forces could be attributed directly to focal adhesions. This enables a mapping of the traction forces to individual focal adhesions

and spatially quantify subcellular distributions of focal-adhesion area, traction force and focal-adhesion stress (defined as the ratio of traction force to corresponding focal adhesion area).

It is of interest to know whether or not micropost rigidity could regulate stem cell lineage commitment, and so it is described that hMSCs plated on micropost arrays with different post heights (L) and exposed to growth medium did not express differentiation markers at any micropost rigidity. However in bipotential differentiation medium supportive of both osteogenic and adipogenic fates (Mcbeath et al 2004; Beningo et al. 2001) after two weeks of induction, it was observed substantial osteogenic and adipogenic differentiation on micropost arrays, indicated by alkaline phosphatase (ALP) activity and formation of lipid droplets (Lip), respectively (Fu et al., 2010). As expected, micropost rigidity shifted the balance of hMSC fates: osteogenic lineage was favored on rigid micropost arrays whereas adipogenic differentiation was enhanced on soft ones. It look micropost rigidity switches hMSCs between osteogenic and adipogenic lineages but the mechanism by which this rigidity-dependent switch occurred is not well understood (Fu et al., 2010).

Cultures of MSCs in hydrogels are widely used in mechanotransduction studies, but the microposts can also be used as another viable option to study MSCs mechanotransduction since they can also mimic different stiffness (to which hMSCs appear to respond) and can be used to track traction forces of individual cells by measuring post bending.

I.3 - Project rationale and experimental approach

I.3.1 - Typical MSCs Isolation

Typically, MSCs are isolated and cultured on polystyrene culture dishes (Secco et al., 2008) and eventually transferred onto compliant substrates after several passages to assess their plasticity in terms of lineage-specific expression markers, as reported in case of osteogenic-, myogenic- or neural-like commitment (Engler et al, 2006).

Nevertheless, MSCs might retain memory (Tse and Engler, 2011) from the extremely high stiffness of polystyrene, possibly restraining their full potential in terms of lineage commitment.

I.3.2 - Durotaxis, Tissue Elasticity and MSCs “memory”

It has been shown that MSCs, even within shallow durotactic gradients, migrate towards the stiffer matrix (durotaxis) and then differentiate into a more contractile cell, but this behavior seems to be hampered by some degree of ‘memory’ that the cells apparently retain from the previous soft environment from which they migrated (Tse and Engler, 2011). MSCs can remain plastic and express differentiation program(s) triggered by stiffness from a region in which they previously resided (Tse and Engler, 2011).

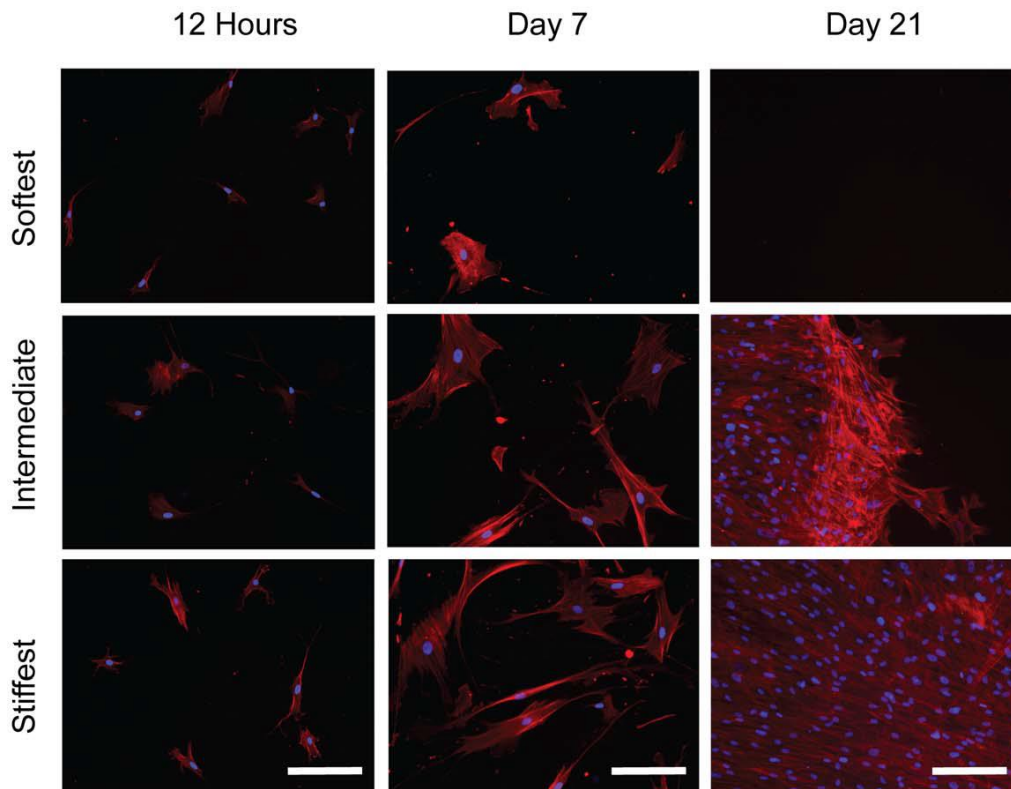


Figure 11 - Images of mitomycin C-treated MSCs on gradient hydrogels (with stiffness gradient, ≈ 1 to 15 kPa) and their spatial distribution. Hoechst 33342 (blue) and phalloidin (red)-stained mitomycin C-treated MSCs plated at 250 cells/cm², illustrate the change in distribution with time. Scale bar is 56.5 μ m. Adapted from Tse and Engler, 2011.

Making a closer approach to the durotaxis, it is described that the actomyosin cytoskeleton maintains polarized morphology and requires tension for durotaxis. Focal adhesion complexes at the leading edge of cells likely establish critical intracellular signaling gradients for durotaxis (Tse and Engler, 2011). It was observed that by 21 days, the center of the hydrogel became locally confluent (Figure 11, right), and because of the mitomycin C treatment (which inhibits cell proliferation), this was in fact created by all cells undergoing directed migration to the stiffest region of the hydrogel (Engler et al. 2006). Durotaxis can also be observed in mitomycin C-treated MSCs plated at higher densities, i.e. 1000 cells/cm², and again a loss of cells at the softest regions and an accumulation of cells at the stiffest regions were observed (Tse and Engler, 2011).

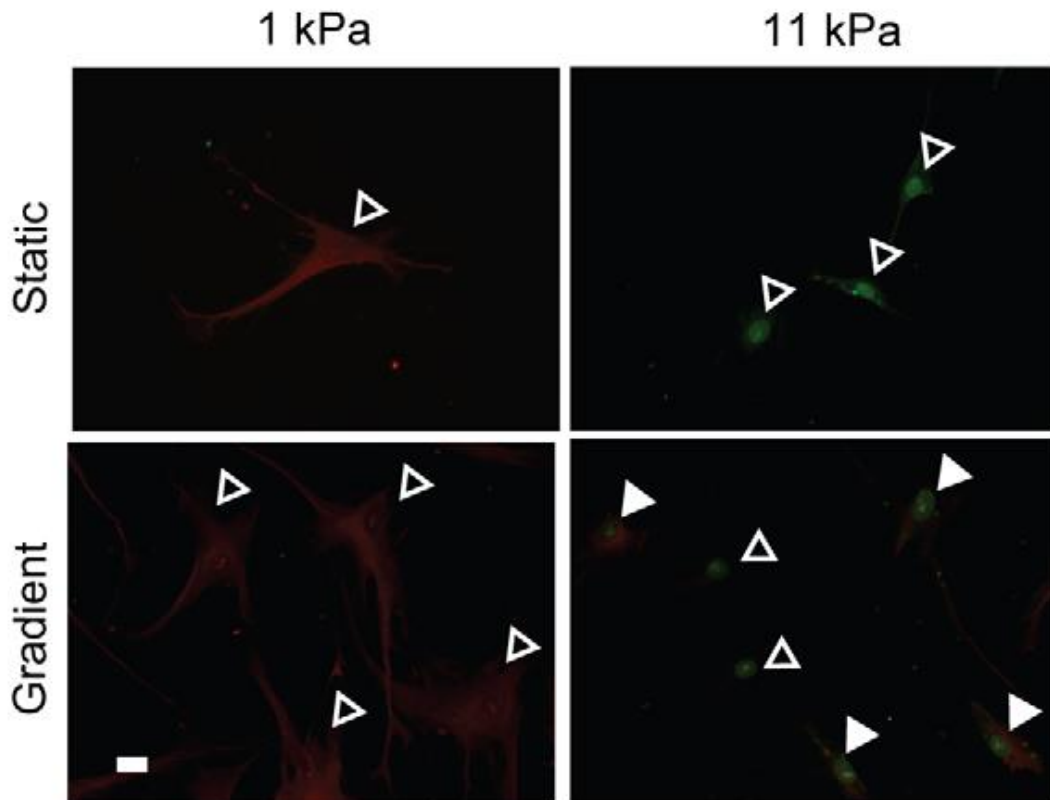


Figure 12 - MSCs cultured on 1 and 11 kPa static (top) and gradient (bottom) hydrogels and stained for B-III- tubulin (red) (neuronal marker) and MyoD (green) (myogenic marker). Open arrowheads indicate cells expressing either B-III- tubulin or MyoD while filled arrowheads indicate doubly stained cells. Adapted from Tse and Engler,, 2011.

To study the “memory” of MSCs, Tse and Engler showed that in static hydrogels, after 7 days, in values of elasticity of 1 and 11 kPa there was expression of B-III tubulin and MyoD-positive MSCs, respectively, and cells remaining on soft regions of gradient hydrogels expressed B-III tubulin (Figure 12, open arrowheads). However, MSCs on the stiffer regions of the gradient displayed a mixed phenotype consisting of cells positive for MyoD alone (open arrowheads) and those also expressing low amounts of B-III tubulin (filled arrowheads)(Figure 12). When B-III tubulin and MyoD fluorescent intensities were quantified and normalized to the non-permissive static hydrogel, i.e. 11 and 1 kPa hydrogels respectively (Figure 13), MSCs on stiffer regions had on average a 3-fold higher B-III tubulin fluorescent intensity versus the control static stiffer hydrogel (11kPa). On the other hand, MSCs on softer regions had less than a 50% difference in MyoD fluorescence when compared to the cells plated on the static hydrogel.

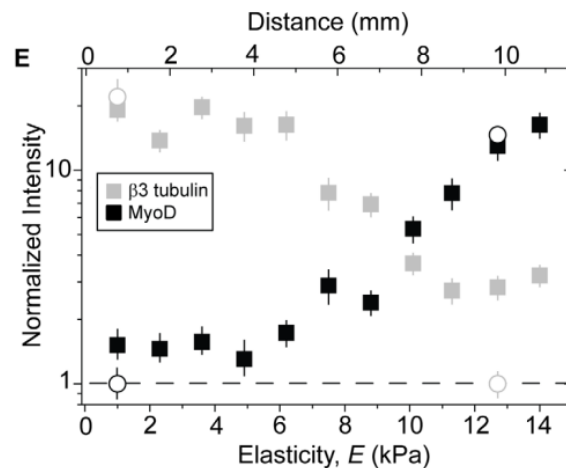


Figure 13 - Quantification of B-III tubulin (grey) and MyoD (black) by MSCs fluorescent intensity on gradient hydrogels (from 1 to 11 kPa, filled squares) and normalized to the non-permissive static hydrogels (1 and 11kPa each and only, open circles). Adapted from Tse and Engler, 2011.

In Figure 13 we can see that B-III tubulin and MyoD intensities were normalized to MSC intensity on static 11 and 1 kPa hydrogels, respectively. The dashed line indicates no change of the proteins in the non-permissive static hydrogels (Tse and Engler, 2011).

This data (Figure 12 and 13) suggests that MSCs can remain plastic and express specific lineage markers triggered by stiffness from a region in which they previously resided, the so called “memory” (Tse and Engler, 2011).

I.3.3 - Effects of the stiffness on the MSCs stemness genes

Stiffness can regulate the differentiation potential of MSCs (Engler et al., 2006; Her et al., 2013; Tse and Engler, 2011). The influence of stiffness on MSCs stemness was also reported (Her, et al. 2013), namely by evaluating how MSCs marker react to stiffness. Using 3-D Col-HA scaffolds of 1 and 10 kPa, hMSCs were cultured for 1 or 2 weeks and then collected for qRT-PCR. From the results, they observed that the expression of MSC stemness genes (including CD73, CD90 and CD105) was down-regulated during culture, suggesting that the hMSCs in soft and stiff substrates started to differentiate under various mechanical stimuli (Figure 14). The gene expression of representative MSC surface markers remained at a low level after 2 weeks of culture. The gene expression level of CD73, CD90, and CD105 in stiff substrate was significantly lower

than that in soft substrate. This suggests that hMSCs in stiff substrate might have entered a differentiated state earlier than those in soft substrate (Her et al, 2013). So to maintain hMSCs in a less differentiated state, softer substrates might be necessary during their isolation and proliferation.

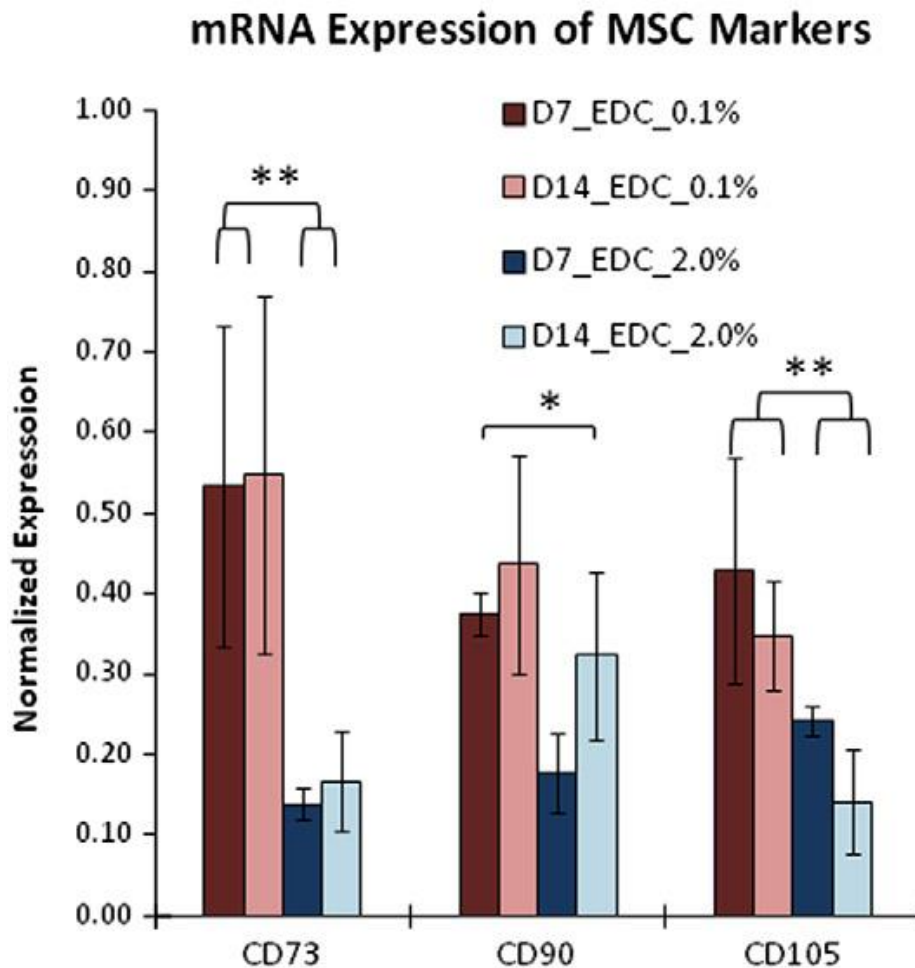


Figure 14 – Graphic represents the results of gene (CD73, CD90 and CD105) expression in MSCs cultured for 7 days (D7) and 14 days (D14) in the Col–HA scaffolds of EDC 0.1% and EDC2.0% which have stiffness of approximately 1 and 10 kPa, respectively, and were defined as soft and stiff substrates, respectively. The results were compared to individual day 1 gene expression levels. Adapted from Her et al., 2013).

I.4 - Objectives

It is of interest to understand what would be the effect of isolating MSCs directly on substrates with stiffness similar to that of neural tissues in terms of their potential to express neural markers.

We propose to isolate and culture human umbilical cord matrix MSCs directly on softer substrates, namely hydrogels compliant with neural tissue (1 to 10KPa) and, as a control, part of the umbilical cord matrix of every sample will be used to isolate MSCs using normal tissue-culture polystyrene plates (the typical isolation and culture protocol) and then transferred onto similar hydrogels after several passages on polystyrene (P1-P5). To study if prolonged culture of MSCs on stiff polystyrene (P2-P5) will restrain their capacity to express neural markers later on or not when compared to isolated cells in the hydrogels. We will then assess the differences in expression levels of specific MSCs markers, but also of makers of neural stem/progenitor cells (nestin) and specific neural lineage markers, such as neuronal (beta-III-tubulin), oligodendroglial (O4) and astroglial (GFAP) markers.

Chapter II - Materials and Methods

II - Materials and methods

II.1 - Materials

II.1.1 - Cell culture

Cell culture dishes were from Corning-Costar. Cell culture Neurobasal[®] medium (1x), MEM-Alpha Medium (1x) and Dubecco's Phosphate Buffered Saline 10x were from Gibco[®]. 0,05% Trypsin-EDTA (1x), Penicillin(10000 units/ml) / Streptomycin (10mg/ml) solution and Fungirone[®] Amphotericin B (250 µg/ml) were from Invitrogen. MSC-qualified Fetal Bovine Serum (FBS) was from Hyclone - Thermo. Medium supplement B27 was from Invitrogen and human recombinant EGF and bFGF were from Peprotech. BSA was from Calbiochem and proteins used to promote cell attachment Collagen type-I(COL-1) from rat tail and human Fibronectin (FN) isolated from plasma were from BD Bioscience and Roche, respectively. All Biological processing was done under sterile conditions using a class-II biosafety vertical air flow cabinet (HeraSafe HS-18, Heraeus). The centrifugation was done using a centrifuge 5810 R from eppendorf. Cells were observed with an Axiovert 40C ZEISS microscope and maintained in a Shel LAB CO₂ Series incubator.

II.1.2 – Polyacrylamide hydrogels

Acrylamide and bis-acrylamide were purchased from Bio-Rad and Applied Chem, respectively. Ammonium persulfate (APS) and dichlorodimethylsilane, Tetramethylethylenediamine (TEMED), NHS (N-Acryloxysuccinimide) and 3-(trimethoxysilyl) propyl methacrylate were from Sigma-Aldrich, Fluka and Santa Cruz Biotechnology, respectively. The gel polymerization system was Mini protean-3 from Bio-Rad.

II.1.3 - Immunocytochemistry

Alexa 488-conjugated donkey anti-mouse and Alexa 568-conjugated goat anti-rabbit antibodies were purchased from Invitrogen. Anti-O4 and anti-Nestin mouse antibodies and anti-Beta-III-Tubulin and anti-GFAP rabbit antibodies are from R&D, Millipore,

Covance and DakoCytomation, respectively. DAPI (4',6-Diamidino-2-phenylindole dihydrochloride) was from Sigma Aldrich.

II.1.4 – Biological material

II.1.4.1 - Umbilical Cord Samples

Cryopreserved Umbilical Cord Fragments were obtained from pre-existing frozen samples from Crioestaminal, S.A and from the Cell Biology Lab (Biocant). All samples were obtained after the informed consent of the donors.

II.1.4.2 - human Mesenchymal Stem Cells (hMSCs)

hMSCs were obtained both by isolation from cryopreserved umbilical cord fragments or from pre-existing lines from the Cell Biology Lab (Biocant), from the previous work of Leite, 2011.

II.2 - Methods

II.2.1 – Isolation of Mesenchymal Stem Cells (MSCs) from Umbilical Cord Fragments (UCFs) in Tissue Culture Plates (TCPs) and Polyacrylamide hydrogels

The isolation of MSCs was adapted from a protocol described by Cristiana O. Leite, 2011. The UCFs normally had to be cut from 5-3 mm long to 1-2 mm long with the help of a scalpel and forceps. Groups of 15 to 30 fragments were transferred to 21 cm² tissue culture plate (TCP) or to 24x50 cm polyacrylamide hydrogels (12cm²) and left to dry for the necessary time (10 to 25 minutes) to promote the attachment of the fragments to the plastic or hydrogel surface. Once the cord fragments were properly attached, MSCs proliferation medium [Alpha-MEM supplemented with 10% MSC-qualified Fetal Bovine Serum (FBS), 1% Penicillin/Streptomycin and 1% Amphotericin B], was added to the culture plate (the hydrogels were also inside a culture plate), until all the fragments were totally immersed. The fragments were then cultured for 15 to 20 days in an incubator at 37°C with 5% CO₂/95% air and 95% humidity, until MSCs were migrating out of the UCM pieces and forming well defined colonies (Reinisch et

al., 2009). Then, the umbilical cord matrix fragments were removed from the tissue culture plate or hydrogels and cells were detached using Trypsin-EDTA 0,05% (or 0,1% for the hydrogels)(Sigma), centrifuged, counted and seeded at the density of 3.000 cells/cm² in MSCs proliferation medium.

II.2.2 - Cell culture

MSCs were maintained as described by Leite, 2011. In detail, cells were passaged by washing with PBS 1x solution followed by dissociation and detachment using 0.05% trypsin-EDTA for 5 min at 37 degrees in the incubator. After, inhibition of trypsin using MSCs proliferation medium (with FBS), cells were centrifuged (at 290g for 5 min), resuspended, counted and seeded on tissue culture dishes at a density of 3000 cells/cm² in MSCs proliferation medium. The cells were maintained in a CO₂ incubator at 37 °C, 5% CO₂/95% air and 95% humidity. The medium was changed every 3 days. When cultured in the hydrogels, cells were left to adhere for 1 hour in a small Proliferation Medium (PM) volume (500µl on 24x50 hydrogels and 80µl on 15x15 hydrogels) and only after, the PM was added until the hydrogels and cells became submersed by PM.

II.2.3 - Cryopreservation of MSCs

Cells were trypsinized and collected to a conical tube. In order to determine the number of cells to freeze per vial, cells were counted and then centrifuged (at 290g for 5 minutes). The medium was then removed and the pellet was resuspended using 1 ml of FBS with 10% DMSO and transferred into cryopreservation vials. The vials were frozen at -80°C overnight in an isopropanol cryo cooler (VWR) and then transferred into a liquid nitrogen tank.

II.2.4 - Phenotypic characterization of UCM-MSCs

The immunophenotypic characterization of UCM-MSCs was performed at passage 2. Cells were treated with accutase, labelled with antibodies against the indicated antigens and analyzed by flow cytometry (FACS Canto II, Becton-Dickinson). The following antibodies were used for the labeling: mouse FITC anti-human CD49e IgG2b,

clone SAM1; mouse Pe-Cy7 anti-human CD13 IgG1, clone WM15; mouse PE anti-human CD73 IgG1, clone AD2; mouse APC anti-human CD90 IgG1, clone 5E10; mouse PO anti-human CD45 IgG1, clone HI30; mouse PB anti-human CD11b IgG1, clone ICRF44; mouse APC-H7 anti-human HLA-DR IgG2a, clone G46-6. The staining and image acquisition and analyze

II.2.5 - Preparation of polyacrylamide hydrogels

Since polyacrylamide hydrogels were polymerized on top of autoclaved glass coverslips (15x15 cm or 24x50 cm), a treatment to allow the establishment of chemical covalent links between the coverslip and the hydrogel using a silane agent was necessary (adapted from Hoffecker et al., 2011).

A dilution of 3-(Trimethoxysilyl) propyl methacrylate in ethanol of 1:200 was made and just before use was added 3% of diluted acetic acid (1:10 glacial acetic acid: water). This solution was placed on top of cleaned coverslips, allowed to react for 3 minutes and then the reactive coverslips were rinsed with ethanol to remove the residual reagent and dried (Hoffecker, et al. 2011).

After the glass coverslips treatment with the silane agent, a saturated solution of N-Acryloxysuccinimide (NHS) was prepared in toluene and kept covered to prevent toluene evaporation. The NHS solution was used in the hydrogel composition to allow the functionalization of the hydrogel surface with covalently bound proteins to allow for cell adherence. Then, the solution of acrylamide, bis-acrylamide, water and TEMED (Tetramethylethylenediamine) was prepared according to Table I. The solution was degassed for 30 min (using a Vacuum Aspiration System from INTEGRA Biosciences). Afterwards, the solutions of NHS and ammonium persulfate (APS) were added to the hydrogel solutions and briefly mixed (adapted from Cretu, et al 2010).

Table I – Composition of the hydrogels solutions - volume added of each reagent (μL) per one milliliter of solution.

Volume (μl)	Gel 1 - 15% Acrylamide/ 0,45% Bis-acrylamide Volume (μl)	Gel 2 - 12,5% Acryl/ 0,37% Bis-acryl (μl)	Gel 3 - 10% Acryl, 0,3% Bis-acryl (μl)	Gel 4 - 3% Acryl, 0,2% Bis-acryl (μl)
Acrylamide 40%	375	312,5	250	75
Bis-acrylamide (2%)	225	185	150	100
NHS	220	220	220	220
APS 10%	3	3	3	3
TEMED 99%	1	1	1	1
Water	176	278,5	376	601

For hydrogels polymerization, each solution (Table I) was poured between the reactive coverslips (which had been previously adsorbed to a back glass with 1 mm spacers) and the outer glass of the gel casting system (Mini protean 3, Bio-Rad). In this platform, the outer glass was treated with a solution of dichlorodimethylsilane in order to turn it hydrophobic and facilitate the polymerization of an hydrogel with a smooth surface and its subsequent detachment from the outer glass (Engler et al., 2004). After polymerization (30 minutes), hydrogels on treated coverslips were washed three times with PBS₇ on a rocker, five minutes per wash. The sterilization was made by exposure to UV light during 30 minutes in an air flow cabinet.

The hydrogels need to be functionalized with proteins that allow cell attachment, since cells do not adhere to polyacrylamide hydrogels and to mimic the extracellular matrix (ECM). The proteins were covalently bond to the surface of the hydrogels by a NHS-ester crosslinking reaction (primary amines with the NHS) on the hydrogel. Collagen type-I (COL-1) and Fibronectin (FN) were diluted in 1x PBS (when referred COL-1 was diluted in 0.2N acid acetic, AA) at a concentration of $2.4\mu\text{g}/\text{cm}^2$ and $10\mu\text{g}/\text{ml}$ respectively. Combination of COL-1/FN was prepared maintaining the concentrations as previously described.

To functionalize the complete surface of the hydrogels its surface were covered with protein solution, using 500 μL or 70 μL for an area of 12 cm^2 (24x50 cm coverslips) or 2.25 cm^2 (15x15 cm coverslips), respectively. The hydrogels were incubated ON at 4 $^{\circ}\text{C}$ to promote the crosslinking of the proteins with NHS and then were washed once with PBS. The unreacted NHS was blocked with 1mg/mL heat-inactivated fatty-acid free BSA (bovine serum albumin) in MEM- α for 30 minutes. BSA solution in PBS (20 mg/ml) was inactivated in a 68 $^{\circ}\text{C}$ water bath for 30 min. Hydrogels were rinsed once with PBS and placed in a plate with MEM- α 4h to equilibrate. Hydrogels were washed with PBS once before the cells were seeded (Adapted from Cretu, et al. 2010).

II.2.6 Differentiation protocols

II.2.6.1 adapted from Engler, et al. 2006

In order to see if the cells isolated in TCPs or in the tunable hydrogels had different plasticity or not, hMSCs were cultured on 10% and 3% acrylamide hydrogels and in TCP. To inhibit proliferation, cells were exposed to mitomycin C (10 mg/ml) for 2 hr and washed three times with media prior to plating. Cells were plated at a 3000 Cells/ cm^2 and let in culture for 7 days. After it, cells were fixated and labelled with anti-O4 and anti-Nestin mouse antibodies and anti-Beta-III-Tubulin and anti-GFAP rabbit antibodies.

II.2.7 - Rheological characterization of polyacrylamide hydrogels

The stiffness of hydrogels was determined by rheology using Kinexus Pro rheometer and rSpace software (Malvern). The hydrogels were prepared and polymerized using a vertical electrophoresis system with a 1mm spacer (Mini-Protean 3, BioRad) and equilibrated overnight in PBS, following a similar protocol as for those used for cell culture, except that the gels were not linked to coverslips neither functionalized with protein. After zeroing the rheometer, each gel was loaded and trimmed on the bottom plate. Then, the gap (distance between the top and bottom plates) was defined as 1mm and fine-tuned to a distance at which the gel was applied a normal force of 0.1N.

Frequency sweeps were performed from 10 to 0.1Hz (3 reads per decade) with a deformation of 2mstrain (amount of deformation, has no units), at 37°C. The elastic modulus (E' , also known as Young's modulus) was calculated using the formula $E' = 2G'(1+\nu)$, where G' is the complex storage modulus measured by the rheometer at 1 Hz and ν is Poisson's ratio, assumed to be 0.5 for materials that do not vary its volume upon stretch, according to the literature (Moore et al., 2010; Saha et al., 2008)

II.2.8 - Immunocytochemistry

Immunocytochemistry was performed on cells cultured on 96 well plates, coverslips or on functionalized hydrogels (15x15 cm and 24x50 cm). The medium was removed, MSCs were washed once with PBS 1x and fixed with 4% paraformaldehyde for 15 minutes at room temperature (RT). The fixing reagent was removed and cells were washed with PBS 1x three times. To stain cells using antibodies, cells were further permeabilized with PBS-Triton 0.1% for 20 minutes and for 5 minutes with PBS-Tween 0.1% and then blocked with 1% BSA in PBS for 30 minutes. The primary antibody (anti O4 and anti Nestin mouse antibodies and anti Beta-III-Tubulin and anti GFAP rabbit antibodies) were diluted in PBS 1%BSA at the appropriated dilution (1:200) and incubated overnight (ON) at 4°C in a humidified atmosphere. The secondary antibodies used to label the primary antibody, Goat anti-rabbit Alexa-568 (1:200) and Donkey anti-mouse Alexa-488 (1:200) were diluted in PBS with 1% BSA and let incubating for 1h at room temperature (RT). DAPI was used for nuclear staining, the cells were incubated with 200ng/ml of DAPI for 5 minutes at RT. For the image acquisition the stained samples were visualized using a Zeiss Axiovert 200M fluorescence microscope using AxioVision release 4.8 software (Zeiss). The Image J software was used to analyze the images.

II.2.9 - Statistical analysis

Statistical analysis was performed by repeated measures one-way ANOVA followed by Tukey's test using the software GraphPad Prism (* $P < 0,05$; ** $P < 0,01$ and *** $P < 0,001$ for statistically significant differences). Values represent mean \pm SEM of at least 3 independent experiments.

Chapter III

Results

III – Results

III.1 – Rheological Characterization of Polyacrylamide Hydrogels

To obtain the stiffness values of the polyacrylamide (PA) hydrogels used in this study, rheological measurements were done using a rheometer. The distinct formulations of polyacrylamide hydrogels tested were the 15% acrylamide (Ac) and 0.45% Bis-acrylamide (Bac) and the 12.5% Ac and 0.37% Bac (the Bis-acrylamide will be omitted from now on and we will refer only to the Ac percentage to simplify). Two additional hydrogels formulations used in this study were already established and characterized in the laboratory (Lourenço, 2012). These results, together with the ones obtained for the new PA hydrogels are summarized in Table II.

Table II - Mean \pm standard deviation (SD) of the Young's modulus (E) (amount of force per unit of area needed to deform the material by a given fractional amount without any permanent deformation) calculated from the shear modulus measured at 1Hz, according to the formula $E = 2G'(1 + \nu)$, where G' is the shear storage modulus measured by the rheometer and ν is the Poisson ratio, assumed to be 0.5 (Moore 2010). Values represent results of measurement of three independent hydrogels ($n=3$). * Hydrogels previously characterized in the laboratory (Lourenço, 2012).

Formulations	G' mean \pm SD (Pa)	$E \pm$ SD (Pa)	$\approx E$ (kPa)
3% Ac + 0.2% Bac*	317.35 \pm 99.78	952.05 \pm 299.34	1
10% Ac + 0.3% Bac*	2210.85 \pm 775.22	6632.55 \pm 2325.65	7
12.5% Ac + 0.37% Bac	3250.00 \pm 363.27	9750.00 \pm 1089.82	10
15% Ac + 0.45% Bac	4003.00 \pm 337.13	12009.00 \pm 1011.39	12

The Young's moduli (stiffness) of the hydrogels (E) were calculated from the G' (shear storage modulus) values measured at 1Hz, 2mstrain and 37°C. E can be calculated using the following formula: $E=2G.(1 + \nu)$, where G is the complex shear storage modulus and ν is the Poisson ratio, assumed to be 0.5 (Moore et al. 2010, Saha et al., 2008). G may be calculated using the formula $G=G'+G''$, where G' is the shear storage modulus and G'' is the shear loss modulus, values which are measured by the rheometer. The shear loss modulus (G'') was ignored for the calculation of E , since its contribution to the overall G (complex shear modulus) is neglectable. The frequency of 1HZ was chosen from a frequency sweep, as described in the literature (Saha et al.,

2008) and also as previously established in the laboratory (Lourenço, 2012). The percentage of acrylamide and bis-acrylamide is correlated with the stiffness of the hydrogels and its increase enhances the Young's moduli (Table I). The hydrogels produced had a range of stiffness between $\approx 12\text{kPa}$ (15% Ac + 0.45% Bac) and $\approx 1\text{kPa}$ (3% Ac + 0.2% Bac) (Table II). Being the soft ones compatible with the range of stiffness described for the brain tissue (Moore et al., 2010) and the stiff ones for better proliferation (Figure 16), as intended.

III.2 – Cell Adhesion to Polyacrylamide Hydrogels functionalized with Collagen I (COL-1)

Collagen I (COL-1) is the most abundant type of collagen found in the ECM of mammalian organisms and it is often used to coat or functionalize substrates for the culture of a variety of cell types (Badylak, 2005). In order to culture human umbilical cord matrix mesenchymal stem cells (hUCM-MSCs) on Polyacrylamide hydrogels functionalized with COL-1, several concentrations of protein were tested to check in which condition cells would show better adherence. Small protein spots ($\approx 2.5\text{mm}^2$) were created on the $\approx 7\text{kPa}$ hydrogels using $2\ \mu\text{l}$ of COL-1 solutions at the following concentrations: $3.125\ \mu\text{g/ml}$, $6.25\ \mu\text{g/ml}$, $12.5\ \mu\text{g/ml}$, $25\ \mu\text{g/ml}$ and $50\ \mu\text{g/ml}$. Phase-contrast microscopy images were taken at day 1 and day 6 after seeding the cells (at a density of $3000\ \text{cells/cm}^2$) to assess the adhesion of MSCs during a period of 6 days (Figure 15). We can clearly see at day 1 that the less the concentration of COL-1 used, the less MSCs initially adhere and that more cells get a round morphology, indicating that these cells did not attach very well to the hydrogels and consequently will detach and/or die. At day 6 we can see that at $3.125\ \mu\text{g/ml}$ there are almost no cells attached; at $6.25\ \mu\text{g/ml}$ there is an area with almost no adherent cells; at $12.50\ \mu\text{g/ml}$ the spot is more homogeneous in terms of adhesion and cells are spread and adherent, but still a lot of free space in the spot when compared with the 25 and $50\ \mu\text{g/ml}$ spots, where we can easily see almost all the spot filled with adherent cells that present a fibroblastoid-like healthy morphology. We selected $50\ \mu\text{g/ml}$ as the most suitable protein concentration, since it promoted the best adhesion from day 1 to day 6.

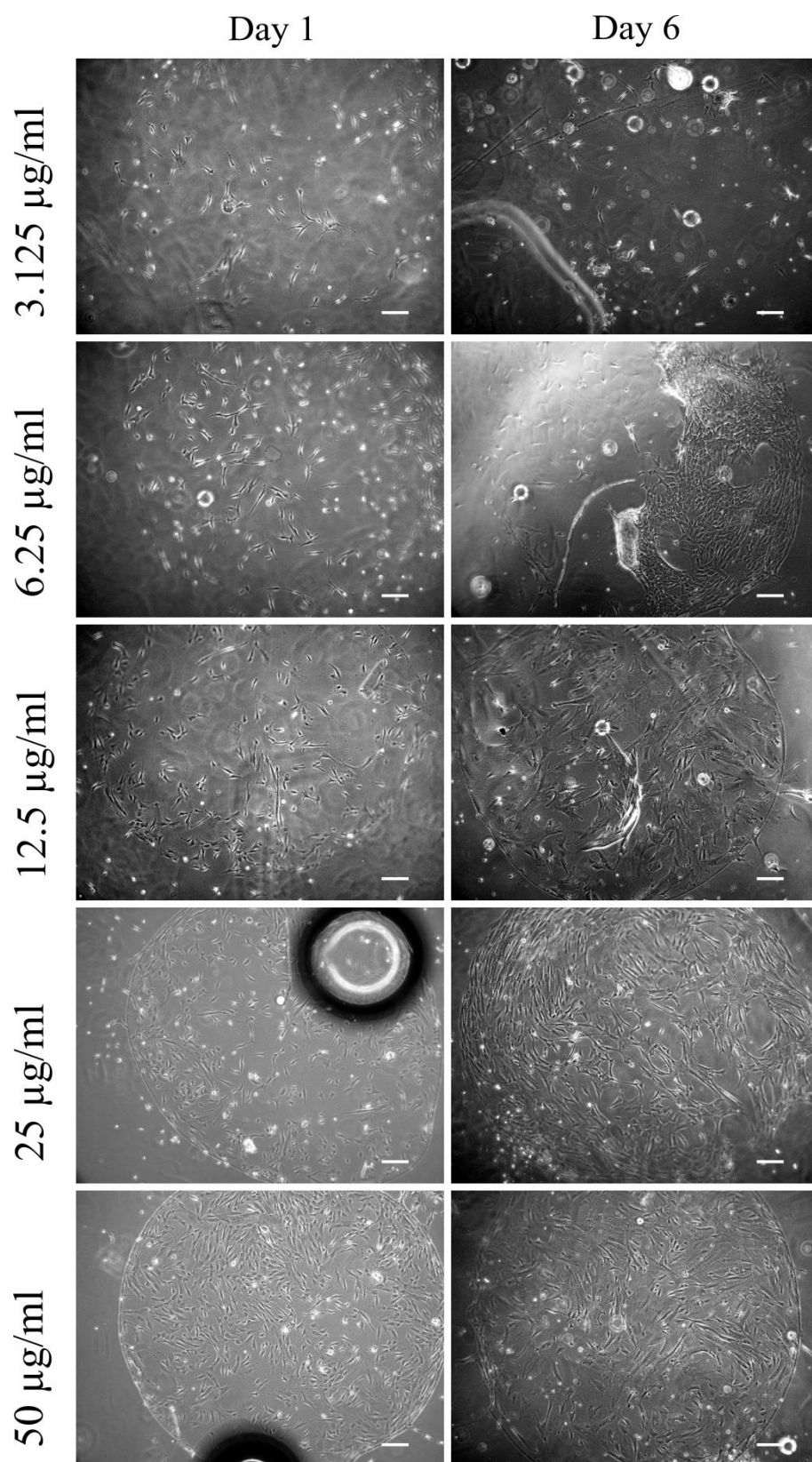


Figure 15 – Representative images of phase-contrast microscopy of cells cultured on ≈ 7 kPa PA hydrogels in which small spots of 2.5 ± 0.5 mm² had been previously functionalized with different COL-1 concentrations (as indicated) to assess cell adhesion 1 and 6 days after seeding. MSCs were plated at 3000 cells/cm² (n=2). Bar represents 100 μm .

III. 3 – hMSCs Proliferation Assay

Mesenchymal stem cells (MSCs) are known to attach and proliferate on polyacrylamide hydrogels functionalized with COL-1 (Engler et al., 2004). Hence, we decided to screen hMSC proliferation on polyacrylamide hydrogels bearing distinct degrees of stiffness (Figure 16). For that, hMSCs were plated at a density of 3000 cells/cm² on hydrogels previously functionalized with 50 µg/ml COL-1 diluted in 1x PBS (PBS) or in acetic acid (AA). Cells were fixed after 1 or 5 days in culture, stained with DAPI and counted using a fluorescence microscope. We observed that proliferation was generally higher on the ≈10 kPa hydrogels, especially when COL-1 was diluted in PBS. Although there were no statistically significant differences, this condition showed slightly increased cell proliferation when compared to plastic (Figure 16). We also observed that in general, proliferation in the ≈7kPa and ≈12kPa hydrogels was normally lower than on plastic, being the lowest in the ≈7kPa hydrogels. In order to proliferate hMSCs in polyacrylamide hydrogels, the ≈10 kPa was selected for subsequent experiments.

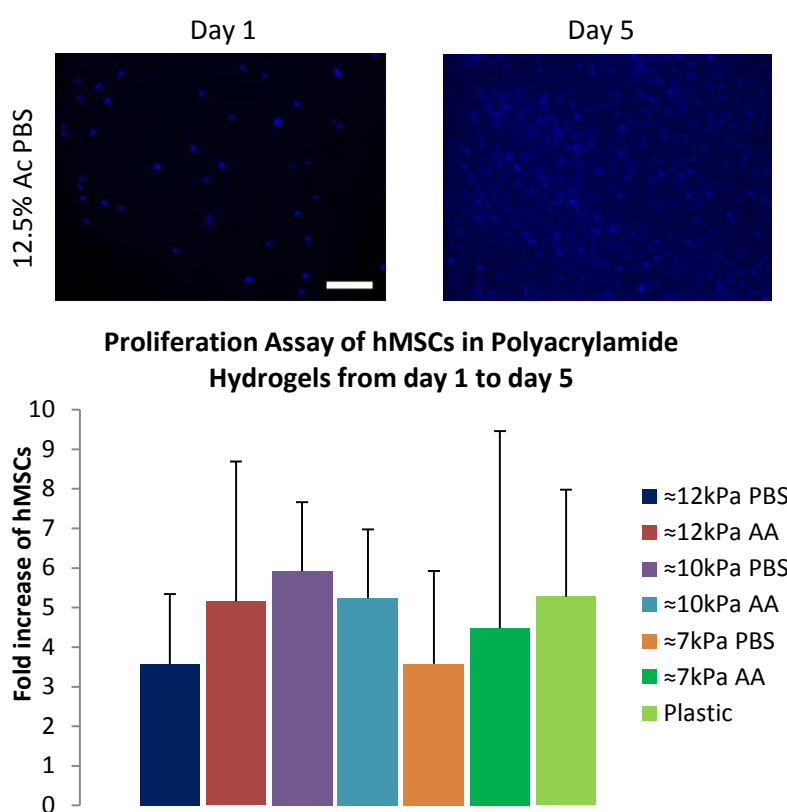


Figure 16 – Left and right upper images: Representative fluorescence microscopy images of hMSCs plated on polyacrylamide hydrogels with 12.5% acrylamide at day 1 (left) and 5 (right) after being fixed and stained with DAPI (in blue). Size bar corresponds to 200µm. Bottom graphic: Proliferation assay of hMSCs in polyacrylamide hydrogels, showing the fold increase of the number of cells from day 1 to day 5 (n=3).

III.4 – Isolation and Proliferation of MSCs from Human Umbilical Cord

Isolation of hMSC from the Wharton Jelly on Polyacrylamide Hydrogels

According to the objectives of this work (I.4), one of the aims was to establish a protocol for the isolation of mesenchymal stem cells from the umbilical cord matrix (UCM) on a soft substrate, namely using functionalized PA hydrogels. To our knowledge this was never done before, and the main objective was to spare the cells from being cultured on stiff tissue-culture polystyrene (TCPs), which we hypothesize that might narrow the plasticity and stemness of MSCs, due to “substrate memory” phenomena that MSCs have been shown to possess (Tse et al., 2011).

Human umbilical cord fragments were plated on different polyacrylamide hydrogels prepared with 10%, 12.5% and 15% Acrylamide (Ac), each bearing distinct degrees of stiffness (Table II). Several formulations were tested, since it was unknown what was the minimum stiffness required for the MSCs to migrate from the umbilical cord fragments to the hydrogels by durotaxis. Furthermore, we tested hydrogels coated only with COL-1 and hydrogels coated with COL-1 plus FN, to find out whether this combination of ECM proteins (COL-1 + FN) might somehow favor the process. What we observed in the first condition (≈ 7 kPa / COL-1) was that hMSCs would migrate from the umbilical cords fragments (UCF) to the ≈ 7 kPa hydrogels in the first week and form small colonies, but after 2 weeks no proliferation was seen and some cells were as if detaching (Figure 17). In the second condition (≈ 10 kPa / COL-1 + FN) it is observed in the first week the migration of hMSCs from the UCF and the formation of small colonies but after 2 week there is no further proliferation of those colonies and in the third condition (≈ 12 kPa / COL-1) happens the same observed in the last 2 conditions. Finally in the last condition (≈ 12 kPa / COL-1 + FN) in the first week there is also migration of hMSCs from the UCF forming colonies but when compared to the others conditions these colonies are more numerous in cells and after the second week we can clearly observe proliferation to the full confluence point (Figure 17). Hence, 12 kPa / COL-1 + FN hydrogels were used onwards for further isolation of hMSCs from umbilical cord fragments.

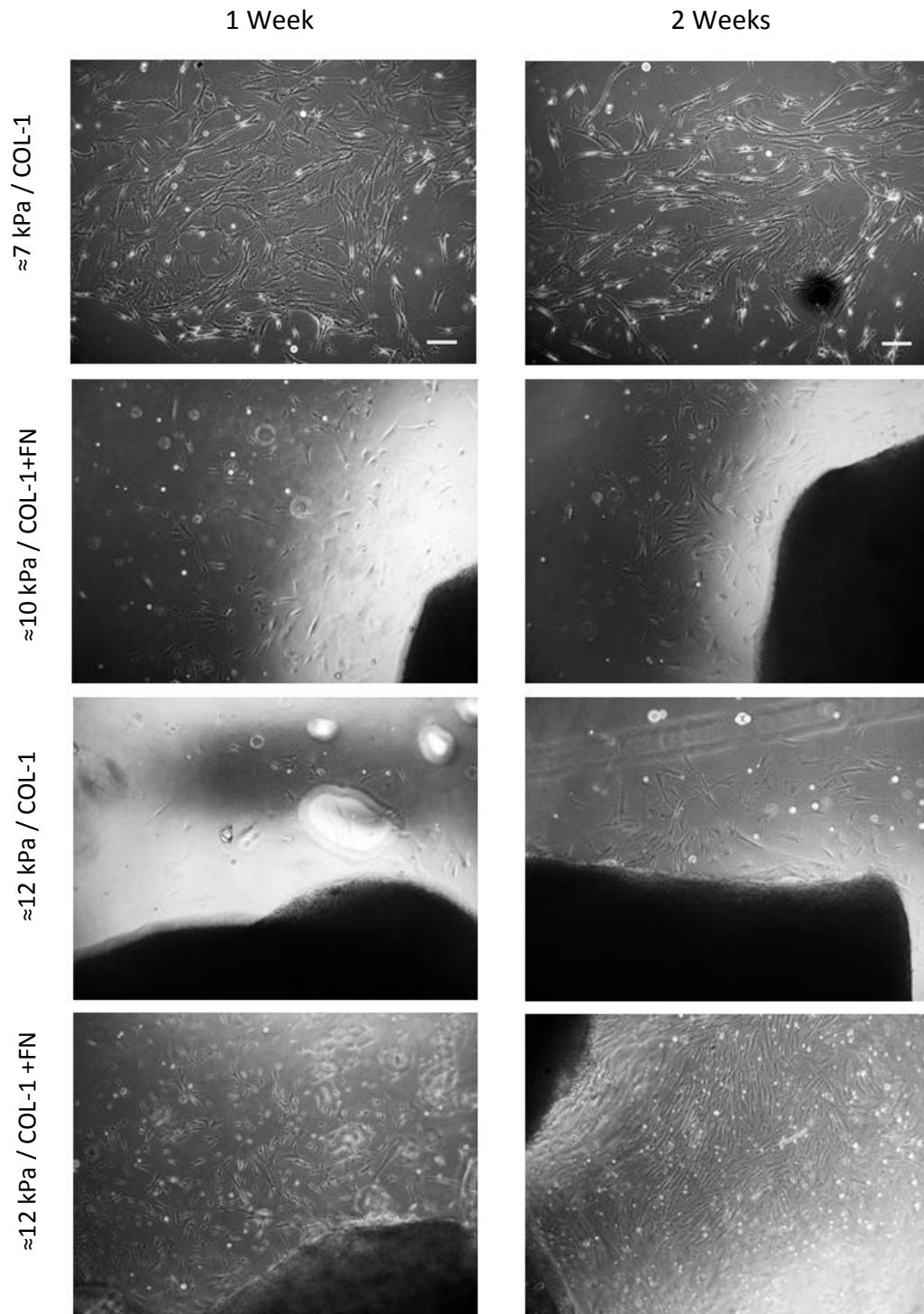


Figure 17 – Colonies of hMSCs isolated in different PA hydrogels from UCM-WJ fragments after 1 week and 2 weeks of fragments plating in the hydrogels with just COL-1 or with COL-1 and FN (n=2). Bar corresponds to 200 μ m.

III.5 - Immunophenotypic characterization of UCM-MSC

In order to determine if the cells isolated from the Wharton's jelly on the PA hydrogels were MSCs, the expression of cell-surface antigens was evaluated at passage 2. As a

control, we used cells from the same biological sample, whose fragments had been plated on TCPs and the resulting cells also cultured on plastic until passage 2. The cells were cultured until subconfluency, detached with accutase and labelled with antibodies against cell surface markers typically used for the characterization of MSCs and analyzed by flow cytometry (Figure 18 and 19). Flow cytometry analysis showed that the cells were strongly positive for CD49e, CD13, CD73 and CD90. In contrast, the cells did not express CD45 (hematopoietic lineage marker), CD11b and HLA-DR. This analysis showed that the MSCs obtained using the two isolation procedures (on TCPs or on the PA hydrogels) have similar phenotypic profiles, consistent with an MSC phenotype (Dominici et al., 2006).

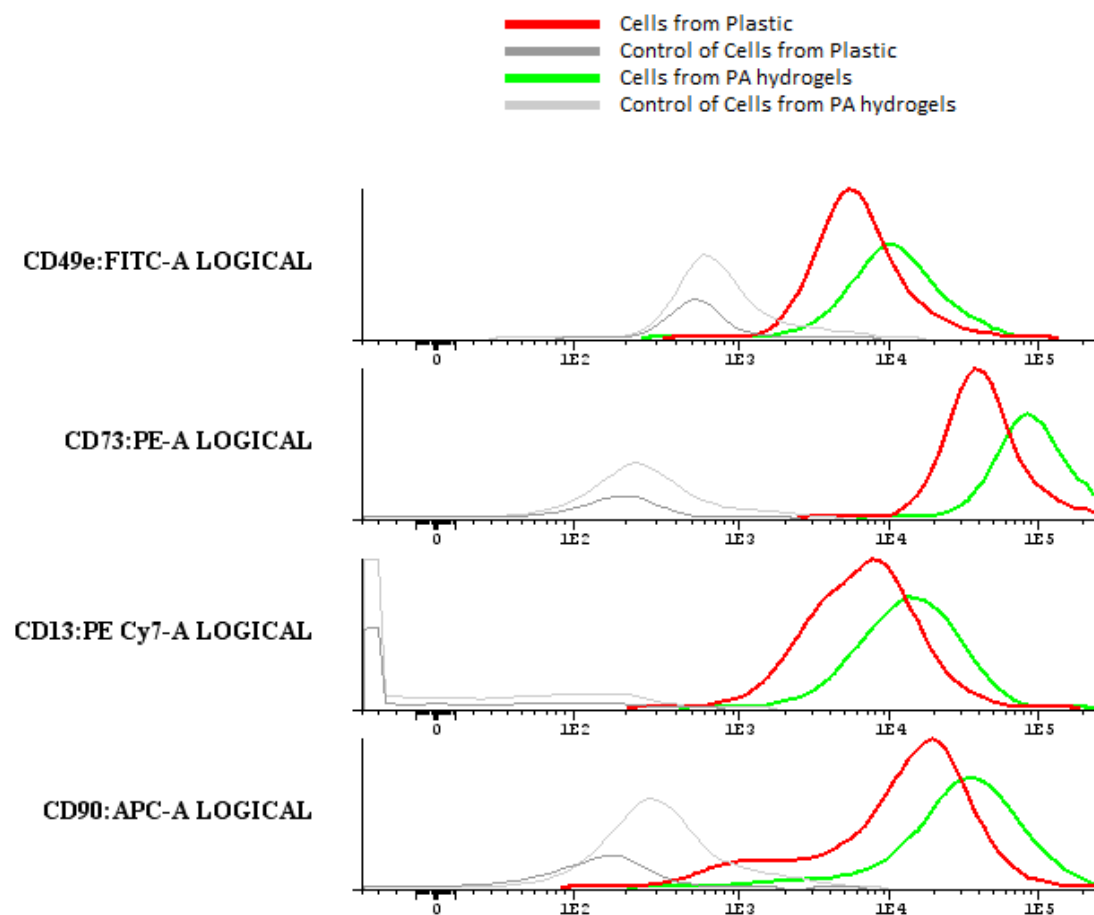


Figure 18 - Immunophenotype of UCM-MSCs. The Y axis is the cell density. The X axis is a logarithmic scale of fluorescence. Cells were detached, labelled with antibodies against the indicated antigens and analyzed by flow cytometry. Cells were positive for CD49e, CD73, CD13 and CD90 (red and green lines) when compared with unlabeled MSCs (dark gray and light gray) for the 2 conditions, both from the PA hydrogels and the Plastic/TCPs (n=1).

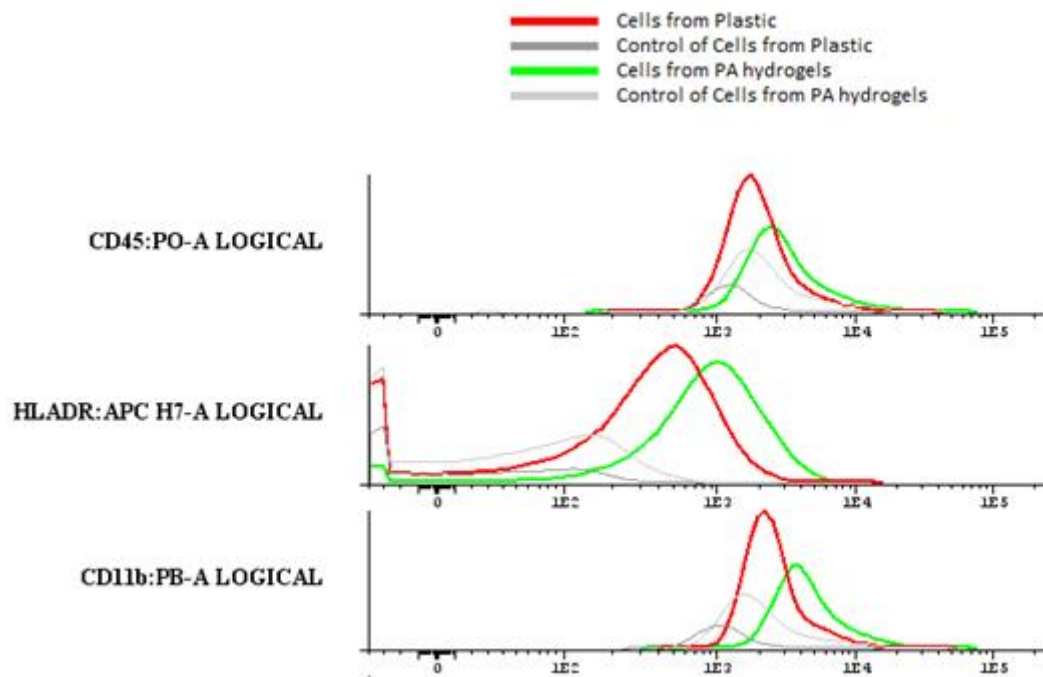


Figure 19 – Immunophenotype of UCM-MSCs. The Y axis is the cell density. The X axis is a logarithmic scale of fluorescence. Cells were detached, labelled with antibodies against the indicated antigens and analyzed by flow cytometry. Cells were negative for CD11b, HLA-DR, CD45 (red and green lines) when compared with unlabelled MSCs (dark gray and light gray) for the 2 conditions, both from the hydrogels and of the Plastic/TCPs (n=1).

After confirming that the cells isolated by both procedures were MSCs, we checked the differences in terms of expression of the MSCs “stemness” markers such as CD49e, CD73, CD13 and CD90 (Table III) and it was observed that the Mean and Median fluorescence intensity of such markers in MSCs isolated on PA hydrogels were clearly higher than those in MSCs isolated on TCPs. Moreover, the coefficient of variation (CV) of the expression levels of these markers was lower in cells obtained from the PA hydrogel when compared to cells obtained from TCPs, suggesting that the population of cells isolated and expanded on the PA hydrogels might be more homogeneous.

Table III: Mean, Median and Coefficient of variation of the Fluorescence values obtained by flow cytometry for the positive MSCs markers (CD49e, CD73, CD13 and CD90) for cells isolated and cultured on PA hydrogels and from TCPs (n=1).

		Markers			
		CD49e:FITC-A	CD73:PE-A	CD13:PE Cy7-A	CD90:APC-A
PA hydrogel Cells	Mean	12790	96650	16759	40724
	Median	10037	84685	13104	31032
	Coefficient of variation	75	52	79	88
TCPs Cells	Mean	7302	46978	8344	17243
	Median	5585	39104	6356	13562
	Coefficient of variation	82	65	90	97

III. 6 – Influence on MSCs specification by matrix elasticity

The second part of this work comprises the assessment of the specification of UCM-MSCs into neural-like cells. The differentiation protocol was adapted from the literature (Engler et al., 2006), from a study where the strong influence of microenvironment stiffness on the specification of stem cells was addressed using MSCs. In that study, cells were directed towards different fates (after inhibition of the cell cycle progression using mitomycin-C), based only on the stiffness of the PA hydrogel that served as substrate to the cells. Importantly, cells subjected to very soft hydrogels (0.1-1 kPa) expressed neuronal lineage markers (like Beta-III tubulin) after 1 week in culture, but not naive mesenchymal stem cells (Engler et al., 2006). In order to determine if cells isolated and expanded on soft matrices (PA hydrogels) show a higher plasticity to differentiate towards neural-like lineages [in a more broad sense, not only neuronal, as addressed by Engler and colleagues (Engler et al., 2006)] than cells isolated and cultured using the conventional methods, we tested MSCs that were isolated and expanded on PA hydrogels and cells isolated and expanded on TCPs (Plastic).

Hence, two experimental setups were used. In the first approach, we used UCM-MSCs previously obtained and characterized in the laboratory (Leite, 2011), that had been expanded on TCPs for 5 passages. The cells were then induced towards neural-like lineages by treating them with mitomycin-C and replating on ~1 kPa PA hydrogels

coated with COL-1 (similar to what was described in Engler et al., 2006), or on TCPs as control. Cells differentiated on TCPs expressed less Beta-III (B-III) tubulin and Nestin (a neuronal marker and an early neural marker, respectively) than the ones differentiated on the PA hydrogels. On the other hand, there were no major differences between cells differentiated on the ≈ 1 kPa and ≈ 7 kPa hydrogels (Figure 20). The expression of the glial markers tested - O4 and GFAP (markers for oligodendrocyte and astrocyte commitment, respectively) - was higher in the 10% PA hydrogels for GFAP, while for O4 it was higher in cells plated on TCPs and 10% PA hydrogels when compared with cells on the softer (3% PA) hydrogels (Figure 21). In general, these results are consistent with results obtained by others using MSCs cultured in 3D hydrogels (Her et al., 2013), where glial fates were also favored by stiffer substrates (~ 10 kPa) and neuronal and neural precursor markers were favored by softer substrates (~ 1 kPa).

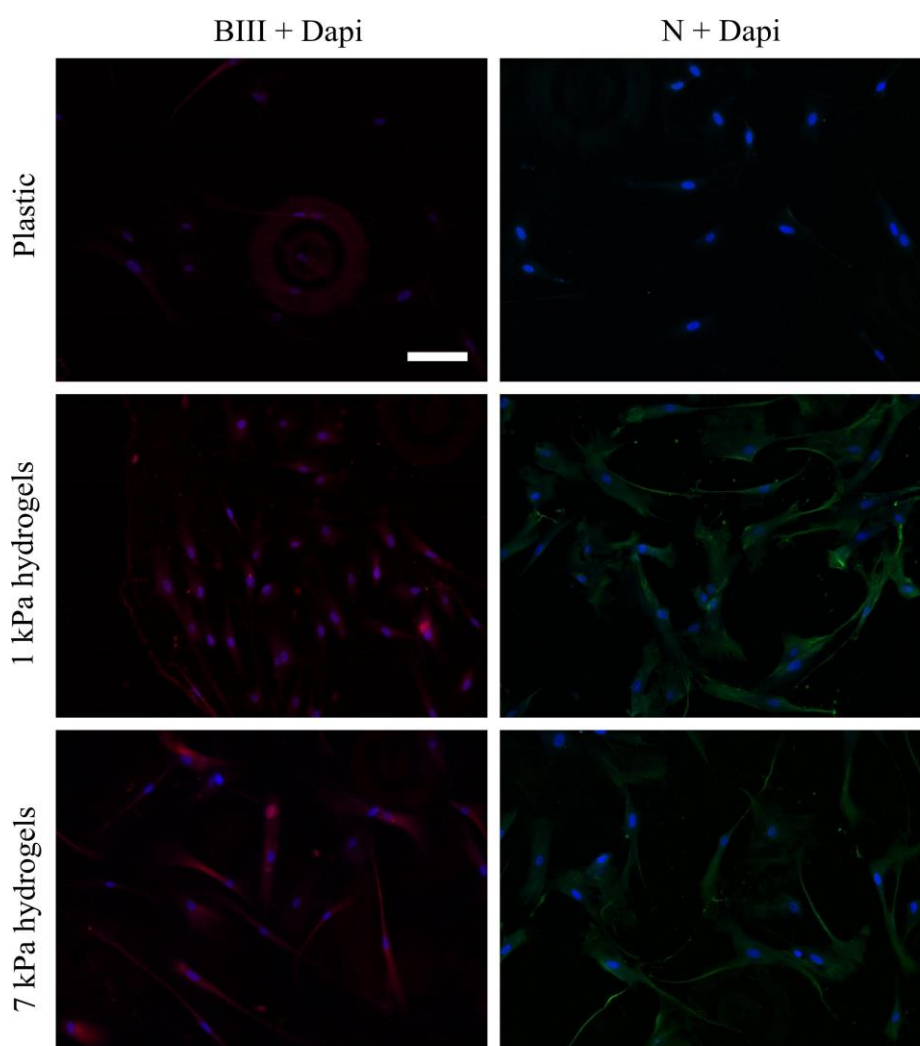


Figure 20 – hMSCs cultured on TCPs (Plastic) and PA hydrogels coated with COL-1 for 7 days after being treated with mitomycin C to inhibit proliferation. Cells were stained with anti-B-III tubulin (red), anti-Nestin antibodies (green) and DAPI (blue). This experiment was performed once (n=1). Bar corresponds to 400 μ m.

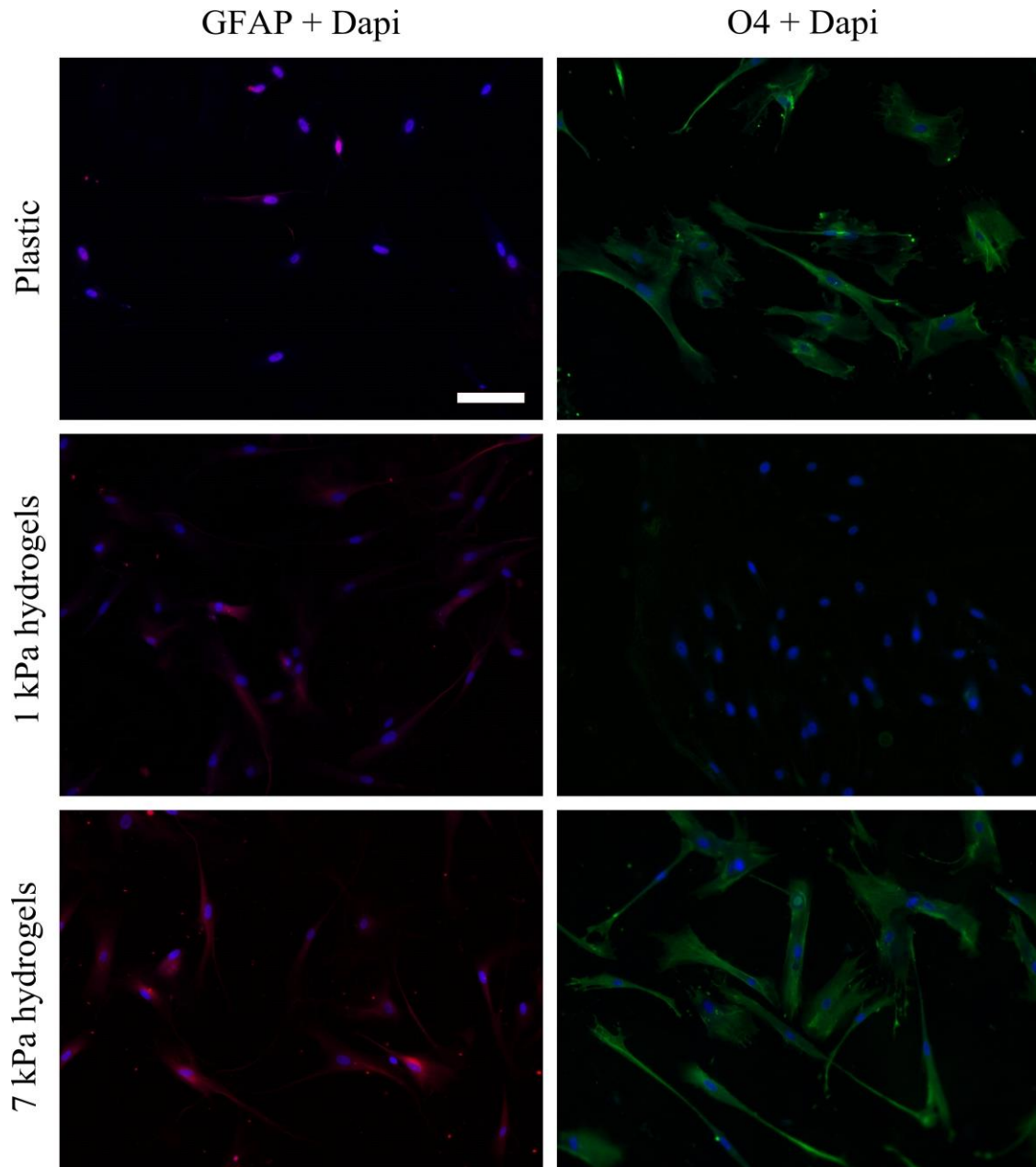


Figure 21- hMSCs cultured on TCPs (Plastic) and PA hydrogels coated with COL-1 for 7 days after being treated with mitomycin C to inhibit proliferation. Cells were stained with anti-GFAP (red), anti-O4 antibodies (green) and DAPI (blue). This experiment was performed once (n=1). Bar corresponds to 400 μ m.

The second experimental setup (and the most innovative part of this work) consisted on isolating MSCs from one biological sample (umbilical cord matrix fragments from one umbilical cord) in parallel on 12 kPa hydrogels and also on plastic, and cells were further expanded for 2 passages on 10 kPa hydrogels or plastic, respectively. After 2 passages, cells were replated and induced to differentiate as described above, on PA

hydrogels of 1 and 7 kPa (for cells originally isolated on hydrogels and on plastic) and on TCPs (for cells originally isolated on plastic), in order to check if the hard stiffness from plastic was affecting the cells isolated even at low passages (P2) when compared to cells that never had contact with hard stiff substrates. All cells were treated with mitomycin C and let on the aforementioned substrates for 7 days with proliferation medium (PM) after plating and then stained for BIII tubulin, Nestin, GFAP and O4. The results (Figure 22 and 23) showed that for Nestin there is not much expression in any of the conditions but there is a slight increase in the cells isolated and cultured on the PA hydrogels only (7kPa hydrogels and 1kPa hydrogels) when compared to those that had contact with the plastic (Plastic, 7kPa hydrogel/TCPs and 1kPa hydrogel/TCPs), being the 7 kPa hydrogels the condition with highest staining. Expression of Beta-III tubulin (BIII) seems higher in the cells cultured on 1 kPa hydrogels, both the ones cultured exclusively on the hydrogels as the ones that were on TCPs (plastic) for 2 passages and then cultured on hydrogels. The expression of BIII tubulin seems to be lower in cells plated exclusively on plastic, with an increase that can be observed when the differentiation took place on hydrogels. In terms of O4, it seems that the cells plated exclusively on the hydrogels (7kPa and 1kPa hydrogels) have more expression when compared to the other cells that had contact with plastic (Plastic, 7kPa and 1kPa Hydrogel/TCPs), being the cells plated exclusively on plastic the ones that show lower O4 expression. Finally, GFAP expression seems to be very similar in all hydrogels being probably the cells plated exclusively on plastic the ones with less expression of GFAP. These results suggest that the expression of the oligodendroglial marker O4 is increased when MSCs are isolated and differentiated on soft substrates (PA hydrogels). This was also observed, to a lesser extent, regarding the expression of nestin. The expression of Beta-III tubulin seems to be enhanced when differentiation takes place on PA hydrogels (soft substrates), but the effect seems to be more independent of the platform used to isolate the cells.

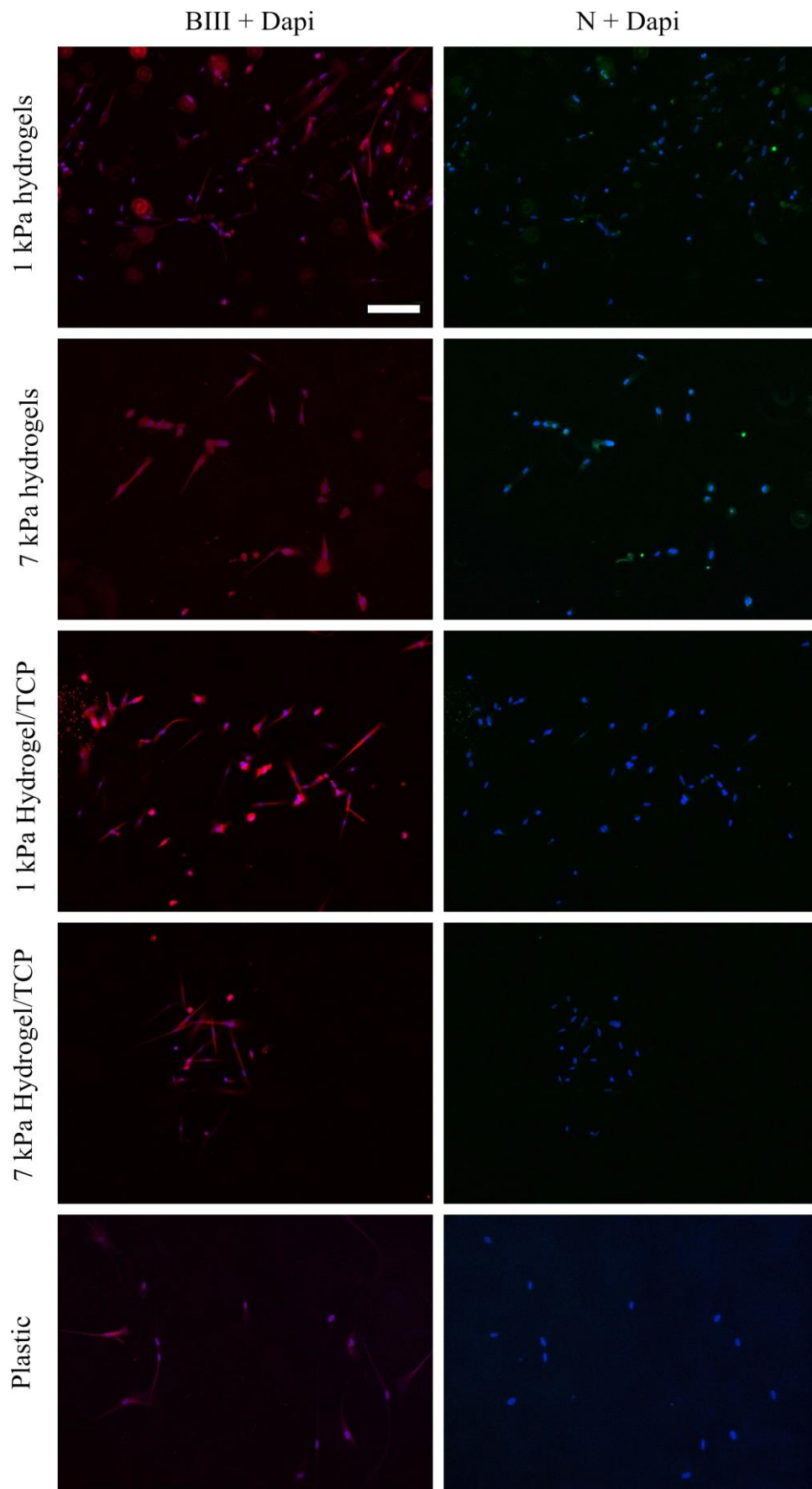


Figure 22 - hMSCs cultured on TCP (Plastic) and PA hydrogels coated with COL-1 for 7 days after being treated with mitomycin C to inhibit proliferation. Cells on the 7kPa hydrogels and 1kPa hydrogels were isolated on 12 kPa hydrogels as mentioned in III.4. Cells were stained with anti-B-III tubulin (red), anti-Nestin antibodies (green) and DAPI (blue). This experiment was performed once (n=1). Bar corresponds to 200 μ m.

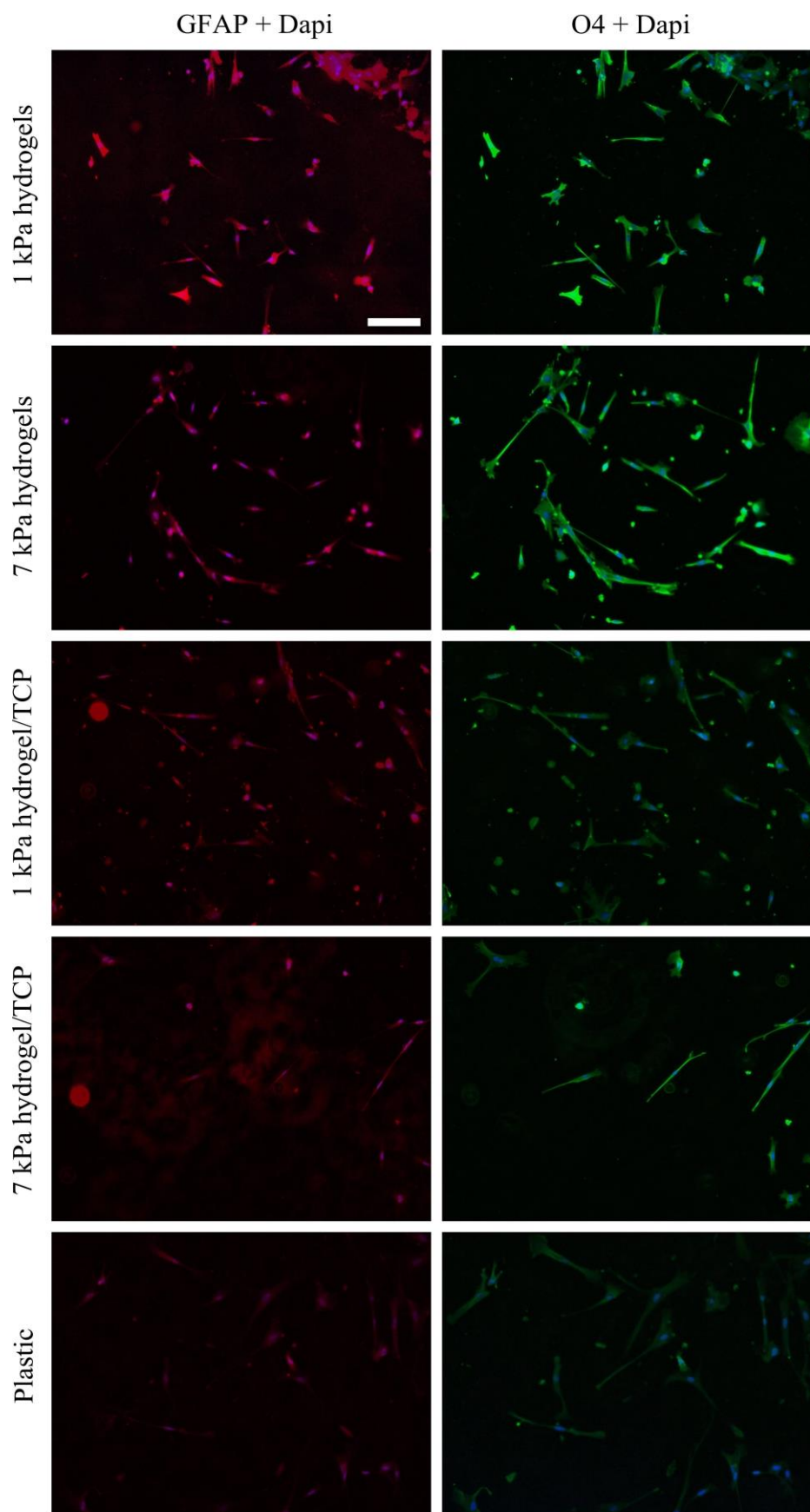


Figure 23 - hMSCs cultured on TCP (Plastic) and PA hydrogels coated with COL-1 for 7 days after being treated with mitomycin C to inhibit proliferation, the cells on the 7kPa hydrogels and 1kPa hydrogels were isolated on 12 kPa hydrogels as mentioned in III.4. Cells were stained with anti-GFAP (red), anti-O4 antibodies (green) and DAPI (blue). This experiment was performed once (n=1) for GFAP and twice for O4 (n=2). Bar corresponds to 200 μ m.

Chapter IV – Discussion and Conclusion

Discussion

MSCs are widely used *in vitro* for purposes of regenerative medicine, tissue engineering or *in vitro* screening due to their ability to proliferate, to form colonies of cells similar to fibroblasts (Friedenstein et al., 1970) and finally due to their multipotent capacity (can differentiate into osteoblasts, chondroblasts, myoblasts and adipocytes) (Prockop, 1997; Nardi and da Silva Meirelles, 2006). MSCs may be isolated from adult tissues such as bone marrow and adipose tissue (Friedenstein et al., 1974; Zuk et al., 2001), but sometimes due to the insufficient amount of cells that can be obtained from these sources, or even because MSCs proliferation frequency and differentiation capacity decrease with age, it is necessary to get alternative sources, such as UCM, UCB and placenta. The collection of these extra-embryonic tissues (that are normally discarded at birth) is both easy and non-harmful to the donor, thus the ethical issues are avoided (Weiss et al., 2006). When working with *in vitro* cell culture, an important factor to keep in mind is the influence of the conditions used to culture such cells and the same is valid when using MSCs, even more when the main objective is cellular differentiation, because cellular response might be hampered by the *in vitro* culture conditions. There is a need to mimic the *in vivo* conditions (to reproduce the cellular *in vivo* environment) to the highest and reasonable extent possible using for example soluble factors, ECM elements and mechanical cues.

In this study, our main focus was to address the effects of changing the biophysical microenvironment (namely stiffness) of hMSCs, by isolating and culturing the cells on stiff TCPs and on soft hydrogels, using the latter to mimic stiffness of human tissues (namely the brain) and its effect on the differentiation potential of hMSCs.

During this work, some components had to be optimized, such as the concentration of the ECM protein COL-1 to which hMSCs would adhere the best, the stiffness in which hUCM-MSCs would migrate from UCF towards the PA hydrogel and the stiffness for higher hMSCs proliferation ratio. Our approach was to identify the conditions that would allow us to isolate hUCM-MSCs on the hydrogels, since it was never done before, to our knowledge, in order to use a differentiation protocol to assess the difference in neural markers when compared to hUCM-MSCs isolated on TCPs (Plastic).

The mechanical aspects of the hydrogels were approached with the objective to obtain PA hydrogels slightly stiffer than those already established in the laboratory, which spun from ~ 1 to ~ 7 kPa (Lourenço, 2012), in order to have a broader range of stiffness where cells could be able to migrate (durotaxis) from the UCM to the hydrogels. We obtained formulations that produced hydrogels presenting Young's moduli ranging from 10kPa and 12kPa (Table II). Both stiffness moduli were useful in this study and used for cell expansion and hUCM-MSCs isolation, respectively.

Initially, hMSCs were plated on PA hydrogels functionalized with COL-1 spots with different concentrations of protein (3.125 $\mu\text{g/ml}$, 6.25 $\mu\text{g/ml}$, 12.5 $\mu\text{g/ml}$, 25 $\mu\text{g/ml}$ and 50 $\mu\text{g/ml}$), to assess in which concentration the adhesion of the hMSCs was more stable (during 6 days). As expected, we observed that the 25 $\mu\text{g/ml}$ and 50 $\mu\text{g/ml}$ were the best conditions with a slight better initial adhesion for the 50 $\mu\text{g/ml}$ condition. Probably because hMSCs in the first 24h are still recovering from the trypsin digestion and do not have all the membrane adhesion proteins recovered, they need a higher protein concentration to adhere on those 24h, thus the best initial results were on 50 $\mu\text{g/ml}$, but after recovering in the 25 $\mu\text{g/ml}$, cells can also stabilize and fill the whole spot, as observed in Figure 15.

As above mentioned, the hMSCs proliferation in different PA hydrogels was assessed, using 7kPa, 10 kPa and 12 kPa hydrogels in order to understand in which stiffness cells would proliferate better for expansion, but still using a range of stiffness much lower than the plastic. When culturing hMSCs for 5 days on the PA hydrogels, we could observe that the 10 kPa hydrogel formulation was the one with higher fold increase in cell number on day 5 compared to day 1, and when comparing to plastic, the cells on the 10 kPa hydrogel with 1xPBS showed even higher proliferation (although not statistically significant). In a general view, the cells on the 7kPa hydrogels were the ones with less fold increase. These results are in agreement with the literature (Winer et al., 2009), since BM-MSCs cultured on substrates with stiffness bellow 7kPa are described to have much less proliferation.

One of our aims was to establish a protocol for the isolation of mesenchymal stem cells from the umbilical cord matrix on a soft substrate, namely using functionalized PA hydrogels. And as it can be observed in Figure 17 it was accomplished but several differences between stiffness and coating were noticed. For the simple purpose of

isolating MSCs on the PA hydrogels, even the softest hydrogels tested (7kPa) would do, but as we need to expand those cells, proliferation of the colonies was necessary. And that was only accomplished on the hardest hydrogels (12 kPa) and with the help of fibronectin. First, when we tried to isolate hUCM-MSCs on PA hydrogels it was observed that the MSCs were migrating from the UCM to all hydrogels but the best colonies were in the 12kPa hydrogels, with a slight improvement comparing to the 10kPa ones. But cells were not proliferating on any COL-1 functionalized hydrogels, so to understand if it was a question of a biochemical ECM-like stimulus that was lacking, we decided to add 1 more ECM protein present in the ECM - fibronectin (FN) - to see if cells would respond better and trigger hMSCs proliferation. Fibronectin, together with collagen-I, is one of the most abundant proteins of the Wharton's jelly ECM (Hao et al., 2013). The FN concentration tested (10 $\mu\text{g/ml}$) was the one already established in the laboratory, known to provide sufficient adherence to MSCs on PA hydrogels (Loureiro, 2012). As we can observe in Figure 17, the presence of fibronectin was a crucial factor for the successful accomplishment of this experiment because it allowed us to isolate hMSC on the 12kPa hydrogels and thus keep the stiffness in low values as intended for better differentiation in a further step. For reasons of time constraints, it was not possible to fully evaluate the MSCs response to FN alone (since in our project only "COL-1" and "COL-1 + FN" was tested). In the future, to better screen the effect of FN in the isolation of hUCM-MSCs on PA hydrogels, we should test 12 kPa PA hydrogels with the 3 conditions: COL-1, COL-1 + FN and FN.

It is interesting to observe that for MSCs that had already been isolated and proliferated *in vitro*, it was sufficient to provide them with COL-1 to achieve proliferation on PA hydrogels, but for *de novo* isolation and proliferation of these cells, the presence of FN was required. It has been described that naive MSCs express high levels of integrin $\alpha 5\beta 1$, the main receptors of adhesion for FN (Goessler et al., 2008) - the CD49e marker expressed by MSCs (Figure 18 and Table III) is an epitope of integrin $\alpha 5$ subunit - and that when stimulated to differentiate this receptor lose expression as if they were no longer needed. Being so, if MSCs stop needing these receptors as they differentiate maybe they do need FN to adhere and proliferate when they are very naive (which is the case of hMSCs isolated in the PA hydrogels). It was also shown that FN plays a role in migration of MSCs via integrin $\alpha 5\beta 1$ (Veevers-Lowe et al., 2011). We

may speculate that FN provides cells with additional migration (Veevers-Lowe et al., 2010) and proliferation stimuli (Hung et al., 2013), activating intracellular signaling pathways that may be required for cell cycle entry. At least in quiescent smooth muscle cells, which are also mesenchymal cells, FN has an important role in promoting the cell cycle entry in the presence of soluble growth factors (Roy et al., 2002). Since it is thought that MSCs on their native tissues are essentially quiescent (namely arrested in the G0 phase of the cell cycle), we may speculate that initiation of proliferation may also have been triggered in our *in vitro* experiments by FN in presence of the soluble growth factors present in the proliferation culture medium.

In order to determine if the cells isolated from the Wharton's jelly on the PA hydrogels were MSCs, the expression of cell-surface antigens was evaluated at passage 2. In Figures 18 and 19 we can see that the cells isolated from UCM on the TCPs and PA express typical MSCs markers. From a close observation it looks like both populations (MSCs isolated from TCPs and PA hydrogels) are very homogeneous, meaning that both isolation processes are very efficient. The population of hMSCs obtained from the PA hydrogels might be more homogeneous than the population obtained from the plastic, as suggested by the lower coefficient of variation obtained by flow cytometry of the first compared to the latter (Table III). When observing the fluorescence obtain by flow cytometry (Table III) for the positive MSCs markers (CD49e, CD73, CD13 and CD90) for cells isolated and cultured on PA hydrogels and from TCPs, it is noticeable that hMSCs isolated from the PA hydrogels have higher mean and median fluorescence intensity values (roughly the double) when compared to hMSCs isolated from plastic. This indicates that hMSCs might be retaining more those typical MSCs markers when isolated and cultured on soft PA hydrogels than on stiff plastic, which is in line with results described in the literature (Her et al., 2013), where gene expression analysis of MSC markers were maintained at higher levels in MSCs differentiated in 3D soft hydrogels than on stiffer hydrogels. These results suggest that maybe MSCs maintain more their properties of naive MSCs on soft than on stiff substrates.

As for our objective to differentiate MSCs in PA hydrogels and assess the differences in the cells isolated on PA hydrogels and on plastic, first we attempted to see if we could repeat what was described in literature (Engler et al., 2006). In the first approach, when we used cells previously obtained and characterized in the laboratory (Leite,

2011) and expanded on TCPs for 5 passages, our results were consistent with what was already described in literature (Engler et al., 2006), that cells differentiated on soft PA hydrogels express more BIII tubulin than the ones plated on plastic (Figure 20). We could also confirm what had been referred, although not much detailed (Engler et al., 2006) that Nestin was also less expressed in cells plated on the plastic when compared to the ones plated in soft PA hydrogels. These results confirm that stiffness itself is capable of stimulating hMSCs to express some neuronal markers. When we looked at glial markers (GFAP and O4) we could observe that the stiffness can also direct MSCs towards a glial-like differentiation (Figure 21), as referred in the literature using 3D hydrogels (Her et al., 2013). Moreover, we observed that there is a small range of stiffness (between 1kPa and 7kPa) from where MSCs can undergo neuronal- or glial-like specification, being the softest substrates (1 kPa) more compliant with neuronal and the hardest substrates (7 kPa) more compliant with glial phenotypes, in agreement with what was described in the literature in promoting the differentiation of neural stem cells into neuronal or glial fates (Saha et al., 2008) and maturation of primary oligodendrocytes (Kippert et al., 2009). To be able to distinguish better in which point the stiffness stimulus favors neuronal- or glial-like differentiation we would need to test more substrates with stiffness between the ones tested. There was also expression of O4 by cells cultured on plastic (Figure 21), which is somehow consistent with the observed tendency of glial markers on stiffer substrates.

In the second experimental setup, looking at B-III tubulin, it is possible to see that cells cultured on plastic have less expression than on hydrogels, but it is not very clear if there is a difference between the cells isolated on PA hydrogels and plated on 1kPa and 7kPa and the cells isolated and plated on plastic until passage 2 and then plated on the 1kPa and 7kPa hydrogels (Figure 22). Nevertheless, the tendency of higher expression of this marker on soft substrates remains. Possibly if cells had been cultured for a longer period on plastic before being transferred onto hydrogels, this difference would have been more evident. The higher levels of B-III tubulin observed on cells that were cultured for only 2 passages on plastic and then plated on hydrogels (Figure 22) comparing with cells from the first experimental setup, which had been in culture already for 5 passages on plastic and then transferred to hydrogels (Figure 20) might be explained by the longer culture period of the latter on a stiff substrate, which

may have caused the cells to lose some plasticity towards neuronal-like lineages, in line with the “memory” issue of MSCs (Tse and Engler, 2011) already discussed in the Introduction section. When observing Nestin, the expression was very low in cells in all conditions. Nevertheless, it could be detected in cells that were isolated, expanded and differentiated on hydrogels (Figure 22), but not in cells isolated and differentiated on plastic, or those isolated on plastic and plated on hydrogels (Figure 22). Although these results require confirmation, they suggest that cells isolated, expanded and differentiated on soft substrates display expression of nestin. It was previously reported that the gene expression levels of neural progenitor markers Nestin and Sox2 were quite low on MSCs differentiated in 3D hydrogels, yet the conditions in which the levels were higher were hydrogels with lower stiffness (~1 kPa rather than ~10 kPa; Her et al., 2013), which is in agreement with our observations. When observing the results for O4 (figure 23) we can see that MSCs isolated on plastic and then cultured on hydrogels have less expression than the ones exclusively plated on hydrogels. This might indicate that MSCs isolated on plastic are more restrained in terms of differentiation and thus can not express O4 as high as the cells isolated on PA hydrogels. In terms of GFAP expression (Figure 23) all cells seem to express the same with maybe a little less expression in the cells plated on plastic.

It will be important to confirm the results regarding the isolation of MSCs on soft substrates and the subsequent differentiation experiments. Also, it will be interesting to follow cells isolated and cultured on hydrogels and on TCPs for several passages (as originally proposed in the project) and assess their differentiation potential along each passage. This was not possible to perform due to time constraints that occurred due to difficulties in identifying the adequate conditions for the isolation of MSCs on hydrogels. Nevertheless, this objective was achieved and to our knowledge, for the first time.

Conclusion

In conclusion, we optimized a new hMSCs isolation protocol for MSCs from UCM, allowing us to obtain naive hMSCs with a more homogenous population when compared to the isolation in TCPs. The PA hydrogels used for the isolation are commonly used in mechanotransduction experiments, but neither this specific formulation neither the isolation of hUCM-MSCs was ever done before in PA hydrogels to the best of our knowledge.

We can conclude that FN together with substrate stiffness have an important role in the initial proliferation impulse of hMSCs when cultured on soft substrates, namely at 10kPa (Figure 17), since on softer hydrogels (7kPa) hUCM-MSCs did not proliferate. Even on hard hydrogels (10kPa) without FN and only COL-1, hMSCs also did not proliferate.

Preliminary results (Figure 18, 19 and Table III) show what appears to be a more naive and more homogenous population of hMSCs isolated and cultured on the PA hydrogels, since the typical MSCs markers studied are more expressed in the hMSCs from PA hydrogels than from TCPs.

Finally, it seems that neural markers (B-III tubulin, Nestin, O4 and GFAP) are more expressed in differentiating hMSCs plated on soft hydrogels than on plastic for hMSCs expanded for 5 passages on plastic. In terms of hMSCs isolated exclusively on PA hydrogels, the differences between these and hMSCs isolated on plastic were not very evident, but O4 seems to be more expressed in cells isolated on soft PA hydrogels.

The added value of this work was discovery of the FN importance for the successful isolation of hUCM-MSCs on soft substrates and more importantly the establishment of a new hMSCs isolation protocol using 12kPa PA hydrogels adding new possibilities for future studies in terms of maintenance and differentiation of hUCM-MSCs *in vitro*, and to dissect the involvement of several important players, such as soluble factors, ECM proteins and mechanotransduction elements.

III. References

- Allingham, J.S., Smith, R., and Rayment, I. (2005). The structural basis of blebbistatin inhibition and specificity for myosin II. *Nat. Struct. Mol. Biol.* 12, 378–379.
- Anzalone, R., M. Lo Iacono, et al. (2010). New emerging potentials for human Wharton's jelly mesenchymal stem cells: immunological features and hepatocyte-like differentiative capacity. *Stem Cells and Development* 19(4): 423-438.
- Aubin, J.E. (1998). *Biochem. Cell Biol.* 76, 899–910.
- Badylak, S.F. (2005). Regenerative medicine and developmental biology: the role of the extracellular matrix. *Anat. Rec. B New Anat.* 287:36- 41.
- Bard, J.B., and Hay, E.D. (1975). The behavior of fibroblasts from the developing avian cornea. Morphology and movement in situ and in vitro. *J. Cell Biol.* 67, 400–418.
- Bauer, N.G. and French-Constant, C. (2009). Physical forces in myelination and repair: a question of balance? *Journal of Biology*: 8:78
- Beningo, K.A., Dembo, M., Kaverina, I., Small, J.V. & Wang, Y.-L. (2001) *J. Cell Biol.* 153, 881–888.
- Berbari, N.F., O'Connor, A.K., Haycraft, C.J., and Yoder, B.K. (2009). The primary cilium as a complex signaling center. *Curr. Biol.* 19, R526–R535.
- Bieback, K., Kern, S., Klüter, H., Eichle, H. (2004). Critical Parameters for the Isolation of Mesenchymal Stem Cells from Umbilical Cord Blood. *Stem Cells* 22(4): 625-634.
- Bisgrove, B.W., and Yost, H.J. (2006). The roles of cilia in developmental disorders and disease. *Development* 133, 4131–4143.
- Black M, Lee V. (1988) Phosphorylation of neurofilament proteins in intact neurons: demonstration of phosphorylation in cell bodies and axons. *J Neurosci*;8:3296–305.
- Burkholder, T. J. (2007). Mechanotransduction in skeletal muscle. *Front. Biosci.* 12, 174- 191.
- Caplan, A. (2009). Why are MSCs therapeutic? New data: new insight. *The Journal of Pathology* 217(2): 318-324.
- Choquet, D., Felsenfeld, D.P., and Sheetz, M.P. (1997). Extracellular matrix rigidity causes strengthening of integrin-cytoskeleton linkages. *Cell* 88, 39–48.
- Christopher S. Chen (2008). *Journal of Cell Science.* doi:10.1242/jcs.0235073285
- Conconi, M., P. Burra, Di Liddo, R., Calore, C., Turetta, M., Bellini, S., Bo, P., Nussdorfer, G.G., Parnigotto, P.P. (2006). CD105(+) cells from Wharton's jelly show in vitro and in vivo myogenic differentiative potential." *INTERNATIONAL JOURNAL OF MOLECULAR MEDICINE* 18: 1089-1096.

Cretu, A., Castagnino, P. & Assoian, R. (2010). Studying the Effects of Matrix Stiffness on Cellular Function using Acrylamide-based Hydrogels. *Journal of Visualized Experiments*, doi:10.3791/2089.

Crouzier, T., Fourel, L., Boudou, T., Albige`s-Rizo, C., and Picart, C. (2011). Presentation of BMP-2 from a soft biopolymeric film unveils its activity on cell adhesion and migration. *Adv. Mater.* 23, H111–H118.

da Silva Meirelles, L., A. Caplan, Nardi, N.B.. (2008). In Search of the In Vivo Identity of Mesenchymal Stem Cells. *Stem Cells* 26(9): 2287-2299.

Davies, P. F., Mundel, T. and Barbee, K. A. (1995). A mechanism for heterogeneous endothelial responses to flow in vivo and in vitro. *J. Biomech.* 28, 1553-1560.

Dehmelt L, Halpain S. (2004). The MAP2/tau family of microtubule-associated proteins. *Genome Biol*;6:204

del Rio, A., Perez-Jimenez, R., Liu, R., Roca-Cusachs, P., Fernandez, J.M., and Sheetz, M.P. (2009). Stretching single talin rod molecules activates vinculin binding. *Science* 323, 638–641.

Discher, D. E., Janmey, P. and Wang, Y. L. (2005). Tissue cells feel and respond to the stiffness of their substrate. *Science* 310, 1139-1143.

Dogterom, M., Kerssemakers, J.W., Romet-Lemonne, G., and Janson, M.E. (2005). Force generation by dynamic microtubules. *Curr. Opin. Cell Biol.* 17, 67–74.

Dominici, M., K. Le Blanc, et al. (2006). Minimal criteria for defining multipotent mesenchymal stromal cells. The International Society for Cellular Therapy position statement. *Cytotherapy* 8(4): 315-317.

Duband, J.L., Nuckolls, G.H., Ishihara, A., Hasegawa, T., Yamada, K.M., Thiery, J.P., and Jacobson, K. (1988). Fibronectin receptor exhibits high lateral mobility in embryonic locomoting cells but is immobile in focal contacts and fibrillar streaks in stationary cells. *J. Cell Biol.* 107, 1385–1396.

Duncan, R. L. and Turner, C. H. (1995). Mechanotransduction and the functional response of bone to mechanical strain. *Calcif. Tissue Int.* 57, 344-358.

Eng LF, Ghirnikar RS, Lee YL. Glial fibrillary acidic protein: GFAP-thirty-one years (1969–2000). *Neurochem Res* 2000;25:1439–51.

Engler, A. J., Griffin, M. a, Sen, S., Bönnemann, C. G., Sweeney, H. L., & Discher, D. E. (2004). Myotubes differentiate optimally on substrates with tissue-like stiffness: pathological implications for soft or stiff microenvironments. *The Journal of cell biology*, 166(6), 877–87. doi:10.1083/jcb.200405004

Engler, A. J., Sen, S., Sweeney, H. L., & Discher, D. E. (2006). Matrix elasticity directs stem cell lineage specification. *Cell*, 126(4), 677–89. doi:10.1016/j.cell.2006.06.044

Eyckmans, J. et al., 2011. A hitchhiker's guide to mechanobiology. *Developmental cell*, 21(1), pp.35–47. Available at: <http://www.ncbi.nlm.nih.gov/pubmed/21763607> [Accessed March 8, 2012].

Friedenstein, A.J. et al. (1974). Precursors for fibroblasts in different populations of hematopoietic cells as detected by the in vitro colony assay method. *Experimental hematology* 2, 83-92.

Goh Jih Her, Hsi-Chin Wu, Ming-Hong Chen, Ming-Yi Chen, Shun-Chih Chang, Tzu-Wei Wan. Control of three-dimensional substrate stiffness to manipulate mesenchymal stem cell fate toward neuronal or glial lineages. *Acta Biomaterialia* 9 (2013) 5170–5180

Hao, H., Chen, G., Liu, J., Ti, D., Zhao, Y., Xu, S., ... Han, W. (2013). Culturing on Wharton's Jelly Extract Delays Mesenchymal Stem Cell Senescence through p53 and p16INK4a/pRb Pathways. *PloS one*, 8(3), e58314. doi:10.1371/journal.pone.0058314

Her, G. J., Wu, H.-C., Chen, M.-H., Chen, M.-Y., Chang, S.-C., & Wang, T.-W. (2013). Control of three-dimensional substrate stiffness to manipulate mesenchymal stem cell fate toward neuronal or glial lineages. *Acta biomaterialia*, 9(2), 5170–80. doi:10.1016/j.actbio.2012.10.012

Hermann, A. et al. Comparative analysis of neuroectodermal differentiation capacity of human bone marrow stromal cells using various conversion protocols. *Journal of neuroscience research* 83, 1502-14 (2006).

Hoffecker, I. T., Guo, W.-h. & Wang, Y.-l. (2011). Assessing the spatial resolution of cellular rigidity sensing using a micropatterned hydrogel–photoresist composite. *Lab on a Chip* 11, 3538, doi:10.1039/c1lc20504h.

Huang, S., Chen, C.S. & Ingber, D.E., 1998. Control of cyclin D1, p27(Kip1), and cell cycle progression in human capillary endothelial cells by cell shape and cytoskeletal tension. *Molecular biology of the cell*, 9(11), pp.3179–93.

Hung, H.-S., Tang, C.-M., Lin, C.-H., Lin, S.-Z., Chu, M.-Y., Sun, W.-S., ... Hsu, S. (2013). Biocompatibility and favorable response of mesenchymal stem cells on fibronectin-gold nanocomposites. *PloS one*, 8(6), e65738. doi:10.1371/journal.pone.0065738

Katsetos CD, Herman MM, Mörk SJ. Class III b-tubulin in human development and cancer. *Cell Motil Cytoskeleton* 2003;55:77–96.

Kippert, A., Fitzner, D., Helenius, J. & Simons, M. (2009). Actomyosin contractility controls cell surface area of oligodendrocytes. *BMC Cell Biology* 10, 71, doi:10.1186/1471-2121-10-71

Lourenço, T. (2012). Regulation of ECM mimetics during oligodendrocytes differentiation in vitro. In *Life Science* (Coimbra: University of Coimbra)

McBeath, R. et al., 2004. Cell shape, cytoskeletal tension, and RhoA regulate stem cell lineage commitment. *Developmental cell*, 6(4), pp.483–95.

Moore, S.W., Roca-Cusachs, P. & Sheetz, M.P., 2010. Stretchy Proteins on Stretchy Substrates: The Important Elements of Integrin-Mediated Rigidity Sensing. *Developmental Cell*, 19(2), pp.194–206.

Owen, M. and A. Friedenstein (1988). Stromal Stem Cells: Marrow-Derived Osteogenic Precursors. *Ciba Foundation Symposium 136 - Cell and Molecular Biology of Vertebrate Hard Tissues*, John Wiley & Sons, Ltd.: 42-60.

Park, K.-S., Y.-S. Lee, et al. (2006). In vitro neuronal and osteogenic differentiation of mesenchymal stem cells from human umbilical cord blood. *J Vet Sci* 7(4): 343-348.

Paszek, M. J. and Weaver, V. M. (2004). The tension mounts: mechanics meets morphogenesis and malignancy. *J. Mammary Gland Biol. Neoplasia* 9, 325-342.

Peyton, S. R. and Putnam, A. J. (2005). Extracellular matrix rigidity governs smooth muscle cell motility in a biphasic fashion. *J. Cell Physiol.* 204, 198-209.

Pelham, R. J., Jr and Wang, Y. (1997). Cell locomotion and focal adhesions are regulated by substrate flexibility. *Proc. Natl. Acad. Sci. USA* 94, 13661-13665.

Prockop, D. (1997). Marrow Stromal Cells as Stem Cells for Nonhematopoietic Tissues. *Science* 276(5309): 71-74.

Reinisch, A. & Strunk, D. (2009). Isolation and animal serum free expansion of human umbilical cord derived mesenchymal stromal cells (MSCs) and endothelial colony forming progenitor cells (ECFCs). *Journal of visualized experiments: JoVE* 4-7 .doi:10.3791/1525

Roy, J., Tran, P. K., Religa, P., Kazi, M., Henderson, B., Lundmark, K., & Hedin, U. (2002). Fibronectin promotes cell cycle entry in smooth muscle cells in primary culture. *Experimental cell research*, 273(2), 169–77. doi:10.1006/excr.2001.5427

Rosen, E.D. & Spiegelman, B.M. (2000). *Annu. Rev. Cell Dev. Biol.* 16, 145–171.

Rutishauser, U. (1984). Developmental biology of a neural cell adhesion molecule. *Nature* 310, 549–554.

Sadoshima, J., Takahashi, T., Jahn, L., and Izumo, S. (1992). Roles of mechano-sensitive ion channels, cytoskeleton, and contractile activity in stretch-induced immediate-early gene expression and hypertrophy of cardiac myocytes. *Proc. Natl. Acad. Sci. USA* 89, 9905–9909.

Saha, K. et al. (2008). Substrate Modulus Directs Neural Stem Cell Behavior. *Biophysical Journal* 95, 4426-4438, doi:10.1529/biophysj.108.132217

Sanchez-Ramos, J., S. Song, et al. (2008). The potential of hematopoietic growth factors for treatment of Alzheimer's disease: a mini-review. *BMC Neuroscience* 9(Suppl 2): S3.

Scherer SS, Braun PE, Grinspan J, Collarini E, Wang DY, Kamholz J. (1994). Differential regulation of the 20,30-cyclic nucleotide 30-phosphodiesterase gene during oligodendrocyte development. *Neuron*;12:1363–75.

Schmidt, C.E., Horwitz, A.F., Lauffenburger, D.A., and Sheetz, M.P. (1993). Integrin-cytoskeletal interactions in migrating fibroblasts are dynamic, asymmetric, and regulated. *J. Cell Biol.* 123, 977–991.

Secco, M., E. Zucconi, et al. (2008). Multipotent Stem Cells from Umbilical Cord: Cord Is Richer than Blood! *Stem Cells* 26(1): 146-150.

Sims, J.R., Karp, S., and Ingber, D.E. (1992). Altering the cellular mechanical force balance results in integrated changes in cell, cytoskeletal and nuclear shape. *J. Cell Sci.* 103, 1215–1222.

Somogyi, K. and Rorth, P. (2004). Evidence for tension-based regulation of *Drosophila* MAL and SRF during invasive cell migration. *Dev. Cell* 7, 85-93.

Sordella, R., Jiang, W., Chen, G. C., Curto, M. and Settleman, J. (2003). Modulation of Rho GTPase signaling regulates a switch between adipogenesis and myogenesis. *Cell* 113, 147-158.

Taghizadeh, R., K. Cetrulo, et al. (2011). Wharton's Jelly stem cells: Future clinical applications. *Placenta* 32, Supplement 4(0): S311-S315.

Takashima, Y., T. Era, et al. (2007). Neuroepithelial Cells Supply an Initial Transient Wave of MSC Differentiation. *Cell* 129(7): 1377-1388.

Veevers-Lowe, J., Ball, S. G., Shuttleworth, A., & Kielty, C. M. (2011). Mesenchymal stem cell migration is regulated by fibronectin through $\alpha 5\beta 1$ -integrin-mediated activation of PDGFR- β and potentiation of growth factor signals. *Journal of cell science*, 124(Pt 8), 1288–300. doi:10.1242/jcs.076935

Wallingford, J.B. (2010). Planar cell polarity signaling, cilia and polarized ciliary beating. *Curr. Opin. Cell Biol.* 22, 597–604.

Wallingford, J.B., and Mitchell, B. (2011). Strange as it may seem: the many links between Wnt signaling, planar cell polarity, and cilia. *Genes Dev.* 25, 201–213.

Wang, H.-S., S.-C. Hung, et al. (2004). Mesenchymal Stem Cells in the Wharton's Jelly of the Human Umbilical Cord. *Stem Cells* 22(7): 1330-1337.

Wang, N., Butler, J.P., and Ingber, D.E. (1993). Mechanotransduction across the cell surface and through the cytoskeleton. *Science* 260, 1124–1127.

Weber, K. T., Jalil, J. E., Janicki, J. S. and Pick, R. (1989). Myocardial collagen remodeling in pressure overload hypertrophy. A case for interstitial heart disease. *Am. J. Hypertens.* 2, 931-940.

Weiss, M. and D. Troyer (2006). "Stem cells in the umbilical cord." *Stem Cell Reviews and Reports* 2(2): 155-162.

Westerhof, N. and O'Rourke, M. F. (1995). Haemodynamic basis for the development of left ventricular failure in systolic hypertension and for its logical therapy. *J. Hypertens.* 13, 943-952.

Winer, Jessamine P.; Janmey, Paul A.; McCormick, Margaret E.; Funaki, Makoto 2009
Goessler, U. R., Bugert, P., Bieback, K., Stern-Straeter, J., Bran, G., Hörmann, K., & Riedel, F. (2008). Integrin expression in stem cells from bone marrow and adipose tissue during chondrogenic differentiation. *International journal of molecular medicine*, 21(3), 271–9.

Wislet-Gendebien, S., G. Hans, et al. (2005). Plasticity of Cultured Mesenchymal Stem Cells: Switch from Nestin-Positive to Excitable Neuron-Like Phenotype. *Stem Cells* 23(3): 392-402.

Wozniak, M.A., Desai, R., Solski, P.A., Der, C.J., and Keely, P.J. (2003). ROCK-generated contractility regulates breast epithelial cell differentiation in response to the physical properties of a three-dimensional collagen matrix. *J. Cell Biol.* 163, 583–595.

Wu, K. H., B. Zhou, et al. (2007). In vitro and in vivo differentiation of human umbilical cord derived stem cells into endothelial cells. *Journal of Cellular Biochemistry* 100(3): 608-616.

Yamada, S., Pokutta, S., Drees, F., Weis, W.I., and Nelson, W.J. (2005). Deconstructing the cadherin-catenin-actin complex. *Cell* 123, 889–901.

Zhang, H.-T., J. Fan, et al. (2010). Human Wharton's jelly cells can be induced to differentiate into growth factor-secreting oligodendrocyte progenitor-like cells. *Differentiation* 79(1): 15-20.

Zeddou, M., A. Briquet, et al. (2010). The umbilical cord matrix is a better source of mesenchymal stem cells (MSC) than the umbilical cord blood. *Cell Biology International* 34(7): 693-701.

Zuk, P., M. Zhu, et al. (2001). Multilineage Cells from Human Adipose Tissue: Implications for Cell-Based Therapies. *Tissue Engineering* 7(2): 211-228.